


Quantization of graphene plasmons

Beatriz A. Ferreira,^{1,2} B. Amorim ,^{1,3,*} A. J. Chaves,⁴ and N. M. R. Peres^{1,2}

¹*Department of Physics, Center of Physics, and QuantaLab, University of Minho, Campus of Gualtar, 4710-057 Braga, Portugal*

²*International Iberian Nanotechnology Laboratory (INL), Av. Mestre José Veiga, 4715-330 Braga, Portugal*

³*CeFEMA, Instituto Superior Técnico, Universidade de Lisboa, Av. Rovisco Pais, 1049-001 Lisboa, Portugal*

⁴*Department of Physics, Instituto Tecnológico de Aeronáutica, DCTA, 12228-900 São José dos Campos, Brazil*



(Received 3 June 2019; revised manuscript received 18 September 2019; accepted 7 February 2020; published 16 March 2020)

In this article we perform the quantization of graphene plasmons using both a macroscopic approach, based on the classical expression for the average electromagnetic energy in a dielectric medium, and a quantum hydrodynamic model, in which graphene electrons are modeled as a charged fluid. Both models allow one to take into account the dispersion in the optical response, with the hydrodynamic model also allowing for the inclusion of the momentum dependence of the optical response (nonlocal effects). Using both methods, the electromagnetic field mode functions, and the respective frequencies, are determined for two different graphene structures. We show how to quantize graphene plasmons, considering that graphene is a dispersive medium, within the local and nonlocal descriptions. It is found that the dispersion of graphene's optical response leads to a nontrivial normalization condition for the mode functions. The obtained mode functions are then used to calculate the decay of an emitter, represented by a dipole, via the excitation of graphene surface plasmon polaritons. The obtained results are compared with the total spontaneous decay rate of the emitter and a near perfect match is found in the relevant spectral range. It is found that nonlocal effects in graphene's conductivity become relevant for the emission rate for small Fermi energies and small distances between the dipole and the graphene sheet.

DOI: [10.1103/PhysRevA.101.033817](https://doi.org/10.1103/PhysRevA.101.033817)

I. INTRODUCTION

In many cases, light-matter interaction can be understood in a semiclassical picture, where matter is quantized and the electromagnetic (EM) field is treated classically. This semiclassical approach holds when the number of photons in the field is large or the light source is coherent. On the other hand, in order to understand the properties of a small number of photons the quantization of the EM field is required. Typical phenomena where the quantization of the EM field is necessary involve entanglement, squeezed light, cavity electrodynamics, interaction of photons with nanomechanical resonators, and near-field radiative effects [1].

Plasmonics emerges as a promising domain to observe quantum effects of the electromagnetic radiation, an example being the Hong-Ou-Mandel interference of plasmons [2]. Many other quantum effects in plasmonics exist, such as the survival of entanglement, particle-wave duality, quantum size effects due to reduced dimensions of metallic nanostructures, quantum tunneling of plasmons (which are simultaneously light and matter), and coupling of surface plasmons to quantum emitters [3–11].

The exploration of quantum effects in plasmonics in unusual spectral ranges, such as the THz and the mid-IR, has been deterred by the poor plasmonic response of noble metals in these regions of the electromagnetic spectrum. However, with the emergence of graphene plasmonics [12,13] the ob-

servation of quantum effects in these yet unexplored spectral regions is a possible prospect. Despite the fact that, at the time of writing, quantum effects involving graphene plasmons remain illusive, the fact that graphene plasmons are characterized by low losses [14–16] boosts the above hope. This has motivated the study of quantized plasmons in graphene, using a model Hamiltonian [17]. The implementation of quantum logic gates using graphene plasmons has also recently been proposed [18]. In addition, graphene plasmons screened by a nearby metal (also called screened or acoustic plasmons) can be confined down to the atomic limit [19], which certainly opens the prospects of finding rich grounds for quantum plasmonics and nonlocal effects [20,21]. Indeed, the idea of developing quantum optics with plasmons has already a long history [22] and quantization of localized plasmons in metallic nanoparticles was recently performed [23,24]. Recently, the quantization of magnon polaritons has also been studied [25].

The development of a quantum theory of the electromagnetic field in the presence of dielectric media has a long history and several approaches have been developed [17,26–37]. These methods are typically based either on the quantization of the macroscopic classic energy [30], on the classical dyadic Green's function for the electric field [31], or on the diagonalization of Hopfield-type Hamiltonians [29]. The quantization of evanescent EM waves [38,39] and of the EM field in the vicinity of a metal [40] have also been considered in the past.

In this paper, we perform the quantization of graphene plasmons, obtaining the plasmonic electromagnetic field mode functions and, importantly, their normalization, when

*amorim.bac@gmail.com, amorim.bruno@fisica.uminho.pt

losses are neglected. These mode functions are then used to study the interaction of graphene plasmons with nearby quantum emitters and determine, in a very intuitive way using Fermi's golden rule, the spontaneous decay rate of the emitter due to plasmon emission. The quantization of graphene plasmons is performed in two ways. (i) A macroscopic approach, which starts from the classical time-averaged energy of the electromagnetic field in a dielectric [27,30,41,42]. This method allows for the inclusion of dispersion in the optical response of graphene. (ii) A hydrodynamic approach, where graphene charge carriers are described in terms of an electronic fluid, which couples to the electromagnetic field [43,44]. The hydrodynamic approach allows not only for the inclusion of dispersion, but also for the inclusion of momentum dependence in the optical response of graphene. A momentum dependent conductivity implies that, in real space, the current response of graphene to an applied electric field is nonlocal. We will, therefore, refer to the momentum dependence of graphene conductivity as nonlocal effects.

The paper is organized as follows. In Sec. II, we present the general macroscopic approach for the quantization of the electromagnetic field in dispersive, lossless media and determine the normalization condition for the mode functions. In Sec. III, we present the quantum hydrodynamic model of graphene. We will see that when nonlocal effects are neglected, the result of the macroscopic approach is recovered. In Sec. IV, the plasmon dispersion relations, mode functions, and mode-normalization constant are obtained for a single graphene layer and for a graphene-metal structure. In Sec. V, we use the quantized plasmon fields to compute the decay rate of a quantum emitter due to the spontaneous emission of plasmons. The plasmon emission rate is compared with the total decay rate of the emitter, which is obtained from the complete dyadic Green's function for the electric field. The role of nonlocal response of graphene is analyzed. Finally, we conclude with Sec. VI, commenting on the obtained results and discussing future research paths. A set of Appendixes detailing the calculations is also presented.

II. MACROSCOPIC QUANTIZATION OF THE PLASMONIC ELECTROMAGNETIC FIELD

In this section, we will describe how the plasmon fields can be quantized using the macroscopic classical energy of the electromagnetic field in a dispersive, lossless dielectric medium. This method was first used in Refs. [27,30,42]. For electric and magnetic fields with a harmonic time dependence,

$$\mathbf{E}(\mathbf{r}, t) = \mathbf{E}_\omega(\mathbf{r})e^{-i\omega t} + \text{c.c.}, \quad (1)$$

$$\mathbf{B}(\mathbf{r}, t) = \mathbf{B}_\omega(\mathbf{r})e^{-i\omega t} + \text{c.c.}, \quad (2)$$

close to a central frequency ω , the time-averaged classical electromagnetic energy in the presence of a dispersive, lossless dielectric is given by [41,45]

$$U_{\text{EM}}(\omega) = \int d^3\mathbf{r} \left(\epsilon_0 \mathbf{E}_\omega^*(\mathbf{r}) \cdot \frac{\partial}{\partial \omega} [\omega \bar{\epsilon}_r(\mathbf{r}, \omega)] \cdot \mathbf{E}_\omega(\mathbf{r}) + \frac{1}{\mu_0} |\mathbf{B}_\omega|^2 \right), \quad (3)$$

where $\bar{\epsilon}_r(\mathbf{r}, \omega)$ is the relative dielectric tensor of the medium and ϵ_0 and μ_0 are, respectively, the vacuum permittivity and permeability. The idea of this method is to promote the above equation to the quantum-mechanical energy of an EM field eigenmode with frequency ω . We will work in the Weyl gauge, in which the scalar potential is set to zero $\phi = 0$, such that the electric and magnetic fields are obtained only from the vector potential \mathbf{A} as

$$\mathbf{E}(\mathbf{r}, t) = -\frac{\partial \mathbf{A}(\mathbf{r}, t)}{\partial t}, \quad (4)$$

$$\mathbf{B}(\mathbf{r}, t) = \nabla \times \mathbf{A}(\mathbf{r}, t). \quad (5)$$

The vector potential is then expanded in modes as

$$\mathbf{A}(\mathbf{r}, t) = \sum_{\lambda} \alpha_{\lambda} e^{-i\omega_{\lambda} t} \mathbf{A}_{\lambda}(\mathbf{r}) + \text{c.c.}, \quad (6)$$

where α_{λ} are amplitudes for the mode λ , with mode function $\mathbf{A}_{\lambda}(\mathbf{r})$ and corresponding frequency ω_{λ} . The mode functions and frequencies are determined by solving the nonlinear eigenvalue problem

$$\nabla \times \nabla \times \mathbf{A}_{\lambda}(\mathbf{r}) = \frac{\omega_{\lambda}^2}{c^2} \bar{\epsilon}_r(\mathbf{r}, \omega_{\lambda}) \cdot \mathbf{A}_{\lambda}(\mathbf{r}), \quad (7)$$

with c vacuum's speed of light, which is just Ampère's law in the dielectric medium for the mode function $\mathbf{A}_{\lambda}(\mathbf{r})$. Next, we assume that the total time-averaged energy for the vector potential Eq. (6) is given by

$$U_{\text{EM}} = \sum_{\lambda} U_{\text{EM}}(\omega_{\lambda}) |\alpha_{\lambda}|^2. \quad (8)$$

The quantization of the theory is achieved by promoting the amplitudes α_{λ} to quantum-mechanical operators

$$\alpha_{\lambda} \rightarrow \sqrt{\frac{\hbar}{2N_{\lambda}\epsilon_0\omega_{\lambda}}} \hat{a}_{\lambda}, \quad (9)$$

$$\alpha_{\lambda}^* \rightarrow \sqrt{\frac{\hbar}{2N_{\lambda}\epsilon_0\omega_{\lambda}}} \hat{a}_{\lambda}^{\dagger}, \quad (10)$$

where, as it will be made more clear in Sec. III, $\hat{a}_{\lambda}^{\dagger}$ (\hat{a}_{λ}) are bosonic creation (annihilation) operators for the quanta of the coupled matter and electromagnetic field: polaritons [26]. If the dielectric function $\bar{\epsilon}_r(\mathbf{r}, \omega)$ describes a metal, the quasi-particles are plasmon polaritons. The bosonic operators obey the usual equal-time commutation relations

$$[\hat{a}_{\lambda}, \hat{a}_{\lambda'}^{\dagger}] = \delta_{\lambda, \lambda'}. \quad (11)$$

N_{λ} is a mode normalization constant, which is determined by demanding that the quantum-mechanical Hamiltonian which is obtained from Eq. (8) by performing the replacement of Eqs. (9) and (10),

$$\hat{H} = \sum_{\lambda} \frac{\hbar U_{\text{EM}}(\omega_{\lambda})}{4N_{\lambda}\epsilon_0\omega_{\lambda}} (\hat{a}_{\lambda}^{\dagger} \hat{a}_{\lambda} + \hat{a}_{\lambda} \hat{a}_{\lambda}^{\dagger}), \quad (12)$$

coincides with the Hamiltonian for a collection of quantum harmonic oscillators

$$\hat{H} = \frac{1}{2} \sum_{\lambda} \hbar \omega_{\lambda} (\hat{a}_{\lambda}^{\dagger} \hat{a}_{\lambda} + \hat{a}_{\lambda} \hat{a}_{\lambda}^{\dagger}). \quad (13)$$

Imposing this condition, we have that the normalization factor is given by $N_\lambda = U_{\text{EM}}(\omega_\lambda)/(2\epsilon_0\omega_\lambda^2)$. Using the mode-function equation (7) to write

$$\begin{aligned} \int d^3\mathbf{r}|\nabla \times \mathbf{A}_\lambda(\mathbf{r})|^2 &= \int d^3\mathbf{r} \mathbf{A}_\lambda^*(\mathbf{r}) \cdot \nabla \times \nabla \times \mathbf{A}_\lambda(\mathbf{r}) \\ &= \frac{\omega_\lambda^2}{c^2} \int d^3\mathbf{r} \mathbf{A}_\lambda^*(\mathbf{r}) \cdot \bar{\epsilon}_r(\mathbf{r}, \omega_\lambda) \cdot \mathbf{A}_\lambda(\mathbf{r}), \end{aligned} \quad (14)$$

the mode normalization factor can be written as

$$N_\lambda = \int d^3\mathbf{r} \mathbf{A}_\lambda^*(\mathbf{r}) \cdot \left(\bar{\epsilon}_r(\mathbf{r}, \omega_\lambda) + \frac{\omega_\lambda}{2} \frac{\partial}{\partial \omega} \bar{\epsilon}_r(\mathbf{r}, \omega_\lambda) \right) \cdot \mathbf{A}_\lambda(\mathbf{r}). \quad (15)$$

Notice that, in the absence of dispersion, the second term vanishes and N_λ reduces to the usual norm in the presence of a position dependent dielectric tensor $\bar{\epsilon}_r(\mathbf{r}, \omega_\lambda)$. For a nonlocal medium, for which the dielectric tensor is a function of two position coordinates, $\bar{\epsilon}_r(\mathbf{r}, \mathbf{r}', \omega)$, the mode normalization generalizes to

$$\begin{aligned} N_\lambda &= \int d^3\mathbf{r} \int d^3\mathbf{r}' \mathbf{A}_\lambda^*(\mathbf{r}) \cdot \left(\bar{\epsilon}_r(\mathbf{r}, \mathbf{r}', \omega_\lambda) \right. \\ &\quad \left. + \frac{\omega_\lambda}{2} \frac{\partial}{\partial \omega} \bar{\epsilon}_r(\mathbf{r}, \mathbf{r}', \omega_\lambda) \right) \cdot \mathbf{A}_\lambda(\mathbf{r}'). \end{aligned} \quad (16)$$

Although this phenomenological method appears to be unjustified, it has actually been shown to be correct for the case when the dielectric is modeled by a Lorentz oscillator [42]. We will see in the next section that Eq. (16) remains valid within a quantum hydrodynamic model of graphene, even when the momentum dependence of the optical response is included. As a matter of fact, Eq. (16) for the mode normalization constant remains valid for any linear optical medium (including effects of dispersion, nonlocality, inhomogeneity, and anisotropy) as long as losses can be neglected [46].

III. PLASMON QUANTIZATION WITHIN A QUANTUM HYDRODYNAMIC MODEL

In this section, we will perform the quantization of graphene surface plasmons employing a hydrodynamic model. The hydrodynamic model provides a classical description of both the electron gas and the electromagnetic field, allowing for the inclusion in a simple and elegant way of nonlocal effects in the optical response of graphene [47]. Nonlocal effects are taken into account by including a pressure term in the Boltzmann equation, that arises due to Pauli's exclusion principle, which leads to a momentum dependent conductivity. A detailed derivation of the hydrodynamic model for graphene can be found in [43,44]. To illustrate the method, we choose the simple case of a single graphene sheet located at the plane $z = 0$, embedded by a static dielectric medium with relative dielectric constant $\bar{\epsilon}_d(\mathbf{r})$.

A. Classical hydrodynamic Lagrangian and Hamiltonian

The classical Lagrangian density for the hydrodynamic model of graphene can be written as

$$\mathcal{L} = \mathcal{L}_{\text{EM}} + \mathcal{L}_{2\text{D hyd}}, \quad (17)$$

where \mathcal{L}_{EM} is the Lagrangian density of the electromagnetic field and $\mathcal{L}_{2\text{D hyd}}$ describes the electronic fluid of graphene and its coupling to the electromagnetic field. Using once again the Weyl gauge, \mathcal{L}_{EM} is given by

$$\mathcal{L}_{\text{EM}} = \frac{\epsilon_0}{2} (\partial_t \mathbf{A}) \cdot \bar{\epsilon}_d \cdot (\partial_t \mathbf{A}) - \frac{1}{2\mu_0} (\nabla \times \mathbf{A})^2, \quad (18)$$

where $\bar{\epsilon}_d(\mathbf{r})$ is allowed to be position dependent, but is frequency independent. Within the hydrodynamic model, the electronic fluid of the graphene layer is described by the fluctuation, n , of the density around the equilibrium density, n_0 , and the displacement vector $\mathbf{v} = (v_x, v_y, 0)$, which should not be confused with the velocity field. In the Weyl gauge, $\mathcal{L}_{2\text{D fluid}}$ is written as [43,44]

$$\begin{aligned} \mathcal{L}_{2\text{D hyd}} &= \delta(z) \left(\frac{1}{2} n_0 m (\partial_t \mathbf{v})^2 + m \beta^2 n \nabla \cdot \mathbf{v} \right. \\ &\quad \left. + \frac{m \beta^2}{2n_0} n^2 - n_0 e \partial_t \mathbf{v} \cdot \mathbf{A} \right), \end{aligned} \quad (19)$$

where the δ function restricts the electronic fluid to the $z = 0$ 2D plane, m is the Drude mass, and β appears from the relation between the degeneracy pressure and the electronic density and depends on the band dispersion for the carriers (see Ref. [43]). Equation (19) follows from a semiclassical Boltzmann's equation approach where the gradient of the degeneracy pressure P acts as an external force. For small density fluctuations, the linearization of P leads to a term proportional to the gradient of the electronic density in the equation of motion: this term corresponds to a diffusive motion. As will be seen in the next subsection, the presence of the diffusion leads to a nonlocal (momentum dependent) electromagnetic response of the fluid. Therefore, β parametrizes the momentum dependence of graphene's conductivity. If we set $\beta = 0$, we recover the local (momentum independent) optical Drude response of graphene. In the approximation of the linear dispersion for graphene electrons, the hydrodynamic parameters are given by [43]: $n_0 = k_F^2/\pi$, $m = \hbar k_F/v_F$, and $\beta^2 = v_F^2/2$, where k_F is the Fermi wave number and v_F the Fermi velocity of graphene. Equation (19) is the 2D equivalent of the Lagrangian for the hydrodynamic model presented in [48].

Using the Euler-Lagrange equations for Eq. (19) with respect to \mathbf{A} , we obtain

$$\nabla \times \mathbf{B} = \frac{1}{c^2} \bar{\epsilon}_d \partial_t \mathbf{E} - \mu_0 n_0 e \partial_t \mathbf{v} \delta(z), \quad (20)$$

which is nothing more than Ampère's law in the presence of a surface current given by

$$\mathbf{J}_s^{\text{hyd}} = -en_0 \partial_t \mathbf{v}. \quad (21)$$

Using the Euler-Lagrange equations for Eq. (19) with respect to the fluid variables n and \mathbf{v} , we obtain the continuity

and Newton's second law with a diffusion term, which read respectively

$$n_0 \nabla \cdot \mathbf{v} + n = 0, \quad (22)$$

$$n_0 m \partial_t^2 \mathbf{v} + m \beta^2 \nabla n = -en_0 \mathbf{E}(z=0), \quad (23)$$

from which we recognize the fluid electronic surface density

$$\rho_s^{\text{hyd}} = -en. \quad (24)$$

Equations (20), (22), and (23) correspond to the linearized hydrodynamic model for graphene [43] (see also [49]).

Notice that Eq. (22) has no dynamics. Therefore, we can use it to eliminate the field n , thus obtaining a new Lagrangian density

$$\mathcal{L}' = \mathcal{L}_{\text{EM}} + \mathcal{L}'_{\text{2D hyd}}, \quad (25)$$

with

$$\mathcal{L}'_{\text{2D hyd}} = \delta(z) \left(\frac{1}{2} n_0 m (\partial_t \mathbf{v})^2 - \frac{1}{2} n_0 m \beta^2 (\nabla \cdot \mathbf{v})^2 - n_0 e \partial_t \mathbf{v} \cdot \mathbf{A} \right). \quad (26)$$

This new Lagrangian is equivalent to Eq. (17) as both lead to the same dynamics. Applying the Euler-Lagrange equations to Eq. (25) with respect to \mathbf{A} leads again to Eq. (20), while the equation obtained for \mathbf{v} reads

$$-m \partial_t^2 \mathbf{v} + m \beta^2 \nabla (\nabla \cdot \mathbf{v}) = e \mathbf{E}(z=0), \quad (27)$$

which can be obtained by combining Eqs. (22) and (23).

From the Lagrangian density Eq. (25), we define the canonical momenta conjugate to the variables \mathbf{A} and \mathbf{v} , respectively, as

$$\mathbf{\Pi} = \frac{\partial \mathcal{L}'}{\partial (\partial_t \mathbf{A})} = \epsilon_0 \bar{\epsilon}_d \partial_t \mathbf{A}, \quad (28)$$

$$\boldsymbol{\pi} = \frac{\partial \mathcal{L}'}{\partial (\partial_t \mathbf{v})} = n_0 m \partial_t \mathbf{v} - n_0 e \mathbf{A}(z=0). \quad (29)$$

In terms of the variables \mathbf{A} , $\mathbf{\Pi}$, \mathbf{v} , and $\boldsymbol{\pi}$, the classical Hamiltonian obtained from Eq. (25) is given by

$$H = \int d^3 \mathbf{r} \left(\frac{1}{2\epsilon_0} \mathbf{\Pi} \cdot \bar{\epsilon}_d^{-1} \cdot \mathbf{\Pi} + \frac{1}{2\mu_0} (\nabla \times \mathbf{A})^2 \right) + \int d^2 \mathbf{x} \left(\frac{[\boldsymbol{\pi} + en_0 \mathbf{A}(z=0)]^2}{2n_0 m} + \frac{1}{2} n_0 m \beta^2 (\nabla \cdot \mathbf{v})^2 \right). \quad (30)$$

B. Canonical quantization of hydrodynamic model

In order to quantize the classical Hamiltonian Eq. (30), we start by introducing the eigenmodes of the coupled electronic fluid plus electromagnetic field. Assuming, we have in-plane translational invariance, we write the vector potential and fluid displacement variables as

$$\mathbf{A}(\mathbf{r}, t) = \frac{1}{\sqrt{S}} \sum_{\mathbf{q}, \lambda} \alpha_{\mathbf{q}, \lambda}(t) e^{i\mathbf{q} \cdot \mathbf{x}} \mathbf{A}_{\mathbf{q}, \lambda}(z) + \text{c.c.}, \quad (31)$$

$$\mathbf{v}(\mathbf{x}, t) = \frac{1}{\sqrt{S}} \sum_{\mathbf{q}, \lambda} \alpha_{\mathbf{q}, \lambda}(t) e^{i\mathbf{q} \cdot \mathbf{x}} \mathbf{v}_{\mathbf{q}, \lambda} + \text{c.c.}, \quad (32)$$

where S is the area of the graphene layer, $\alpha_{\mathbf{q}, \lambda}(t) = \alpha_{\mathbf{q}, \lambda} e^{-i\omega_{\mathbf{q}, \lambda} t}$ are mode amplitudes, with $\omega_{\mathbf{q}, \lambda}$ the mode frequency, and $\mathbf{A}_{\mathbf{q}, \lambda}(z)$ and $\mathbf{v}_{\mathbf{q}, \lambda}$ are mode functions, which, following from Eqs. (20) and (27), obey the equations

$$\left[\omega_{\mathbf{q}, \lambda}^2 \epsilon_0 \bar{\epsilon}_d(z) - \frac{1}{\mu_0} D_{\mathbf{q}} \times D_{\mathbf{q}} \times \right] \mathbf{A}_{\mathbf{q}, \lambda}(z) = -i\omega_{\mathbf{q}, \lambda} \delta(z) en_0 \mathbf{v}_{\mathbf{q}, \lambda}, \quad (33)$$

$$mn_0 [\omega_{\mathbf{q}, \lambda}^2 - \beta^2 \mathbf{q} \otimes \mathbf{q}] \mathbf{v}_{\mathbf{q}, \lambda} = i\omega_{\mathbf{q}, \lambda} en_0 \mathbf{A}_{\mathbf{q}, \lambda}(0), \quad (34)$$

where we defined the differential operator $D_{\mathbf{q}} = i\mathbf{q} + \hat{\mathbf{z}} \partial_z$.

From Eq. (34), we can write

$$\mathbf{v}_{\mathbf{q}, \lambda} = \frac{1}{en_0} \bar{\sigma}_g^{\text{hyd}}(\mathbf{q}, \omega_{\mathbf{q}, \lambda}) \cdot \mathbf{A}_{\mathbf{q}, \lambda}(0), \quad (35)$$

where $\bar{\sigma}_g^{\text{hyd}}(\mathbf{q}, \omega)$ is the conductivity within the hydrodynamic model, which we separate into transverse and longitudinal components as

$$\bar{\sigma}_g^{\text{hyd}}(\mathbf{q}, \omega) = \sigma_{g,T}^{\text{hyd}}(\mathbf{q}, \omega) \left(\bar{\mathbf{1}} - \frac{\mathbf{q} \otimes \mathbf{q}}{q^2} \right) + \sigma_{g,L}^{\text{hyd}}(\mathbf{q}, \omega) \frac{\mathbf{q} \otimes \mathbf{q}}{q^2}, \quad (36)$$

respectively given by

$$\sigma_{g,T}^{\text{hyd}}(\mathbf{q}, \omega) = D \frac{i}{\omega}, \quad (37)$$

$$\sigma_{g,L}^{\text{hyd}}(\mathbf{q}, \omega) = D \frac{i\omega}{\omega^2 - \beta^2 q^2}, \quad (38)$$

where we identify $D = e^2 n_0 / m$ as the Drude weight, which for graphene is given by $D = e^2 E_F / (\pi \hbar^2)$ [50]. Notice that, if we take $\beta = 0$, the conductivity becomes momentum independent (and therefore local in real space), and we recover the Drude model [51]. Inserting Eq. (35) into Eq. (33), we obtain

$$D_{\mathbf{q}} \times D_{\mathbf{q}} \times \mathbf{A}_{\mathbf{q}, \lambda}(z) = \frac{\omega_{\mathbf{q}, \lambda}^2}{c^2} \bar{\epsilon}_r(\mathbf{q}, z, \omega_{\mathbf{q}, \lambda}) \mathbf{A}_{\mathbf{q}, \lambda}(z), \quad (39)$$

with the dielectric function, including screening by graphene electrons, being given by

$$\bar{\epsilon}_r(\mathbf{q}, z, \omega) = \bar{\epsilon}_d(z) + \frac{i}{\epsilon_0 \omega} \bar{\sigma}_g^{\text{hyd}}(\mathbf{q}, \omega) \delta(z), \quad (40)$$

in agreement with Eq. (7).

Inserting the expansions (31) and (32) into Eq. (30), and using the orthogonality properties of the mode functions $[\mathbf{A}_{\mathbf{q}, \lambda}(z), \mathbf{v}_{\mathbf{q}, \lambda}]$ (see Appendix A) it is possible to write the Hamiltonian for the hydrodynamic model as

$$H = \frac{1}{2} \sum_{\mathbf{q}, \lambda} 2\omega_{\mathbf{q}, \lambda}^2 \epsilon_0 N_{\mathbf{q}, \lambda} \alpha_{\mathbf{q}, \lambda}^* \alpha_{\mathbf{q}, \lambda} + \text{c.c.}, \quad (41)$$

with the mode normalization constant, $N_{\mathbf{q}, \lambda}$, given by

$$N_{\mathbf{q}, \lambda} = \int dz \mathbf{A}_{\mathbf{q}, \lambda}^*(z) \cdot \bar{\epsilon}_d(z) \cdot \mathbf{A}_{\mathbf{q}, \lambda}(z) + \frac{n_0 m}{\epsilon_0} \mathbf{v}_{\mathbf{q}, \lambda}^* \cdot \mathbf{v}_{\mathbf{q}, \lambda} + \frac{ien_0}{2\epsilon_0 \omega_{\mathbf{q}, \lambda}} [\mathbf{A}_{\mathbf{q}, \lambda}^*(0) \cdot \mathbf{v}_{\mathbf{q}, \lambda} - \mathbf{v}_{\mathbf{q}, \lambda}^* \cdot \mathbf{A}_{\mathbf{q}, \lambda}(0)]. \quad (42)$$

Promoting the mode amplitudes to quantum-mechanical operators as

$$\alpha_{\mathbf{q},\lambda}^*(t) \rightarrow \sqrt{\frac{\hbar}{2\epsilon_0\omega_{\mathbf{q},\lambda}N_{\mathbf{q},\lambda}}} \hat{a}_{\mathbf{q},\lambda}^\dagger(t), \quad (43)$$

$$\alpha_{\mathbf{q},\lambda}(t) \rightarrow \sqrt{\frac{\hbar}{2\epsilon_0\omega_{\mathbf{q},\lambda}N_{\mathbf{q},\lambda}}} \hat{a}_{\mathbf{q},\lambda}(t), \quad (44)$$

where $\hat{a}_{\mathbf{q},\lambda}^\dagger$ ($\hat{a}_{\mathbf{q},\lambda}$) are plasmon-polariton creation (annihilation) operators, satisfying the usual equal-time commutation relations Eq. (11), the quantum Hamiltonian for the hydrodynamic model is given by

$$\hat{H} = \frac{1}{2} \sum_{\mathbf{q},\lambda} \hbar\omega_{\mathbf{q},\lambda} [\hat{a}_{\mathbf{q},\lambda}^\dagger \hat{a}_{\mathbf{q},\lambda} + \hat{a}_{\mathbf{q},\lambda} \hat{a}_{\mathbf{q},\lambda}^\dagger]. \quad (45)$$

We will now see that Eq. (42) can be recast in the same form as Eq. (16). In order to do so, we use Eq. (35) which allows us to write Eq. (42) as

$$N_{\mathbf{q},\lambda} = \int dz \mathbf{A}_{\mathbf{q},\lambda}^*(z) \cdot \bar{\epsilon}_d(z) \cdot \mathbf{A}_{\mathbf{q},\lambda}(z) + \frac{e^2 n_0}{\epsilon_0 m} \frac{\beta q^2}{(\omega^2 - \beta q^2)^2} \mathbf{A}_{\mathbf{q},\lambda}^*(0) \cdot \frac{\mathbf{q} \otimes \mathbf{q}}{q^2} \cdot \mathbf{A}_{\mathbf{q},\lambda}(0). \quad (46)$$

It is easy to see that the above equation can also be written as

$$N_{\mathbf{q},\lambda} = \int dz \mathbf{A}_{\mathbf{q},\lambda}^*(z) \cdot \left(\bar{\epsilon}_r(\mathbf{q}, z, \omega_\lambda) + \frac{\omega_\lambda}{2} \frac{\partial}{\partial \omega} \bar{\epsilon}_r(\mathbf{q}, z, \omega) \Big|_{\omega=\omega_\lambda} \right) \cdot \mathbf{A}_{\mathbf{q},\lambda}(z), \quad (47)$$

with $\bar{\epsilon}_r(\mathbf{q}, z, \omega)$ given by Eq. (40). The above equation is equivalent to Eq. (16), if we identify $\mathbf{A}_{\mathbf{q},\lambda}(\mathbf{r}) = e^{i\mathbf{q}\cdot\mathbf{x}} \mathbf{A}_{\mathbf{q},\lambda}(z) / \sqrt{S}$. In terms of the conductivity of graphene, the plasmon mode normalization constant can be written as

$$N_{\mathbf{q},\text{sp}} = \int dz \epsilon_d(z) \mathbf{A}_{\mathbf{q},\text{sp}}^*(z) \cdot \mathbf{A}_{\mathbf{q},\text{sp}}(z) + \frac{i}{2\epsilon_0\omega_{\mathbf{q},\lambda}} \mathbf{A}_{\mathbf{q},\text{sp}}^*(0) \cdot \frac{\partial}{\partial \omega} [\omega \bar{\sigma}_g^{\text{hyd}}(\mathbf{q}, \omega)]_{\omega=\omega_{\mathbf{q},\text{sp}}} \cdot \mathbf{A}_{\mathbf{q},\text{sp}}(0). \quad (48)$$

Notice that this expression for the mode normalization constant differs from the one in Refs. [17,52].

IV. DISPERSION RELATIONS AND MODE FUNCTIONS OF GRAPHENE PLASMON IN TWO DIFFERENT STRUCTURES

We now wish to determine the dispersion relation and mode functions of graphene plasmons in two different structures (see Fig. 1): a single graphene layer and a graphene sheet in the vicinity of a perfect metal. As in the previous section, we make use of the in-plane translational invariance of the structures being considered. Therefore, the nonlinear eigenvalue problem for the mode functions, Eq. (7), can be written as

$$D_{\mathbf{q}} \times D_{\mathbf{q}} \times \mathbf{A}_{\mathbf{q},\lambda}(z) = \frac{\omega_{\mathbf{q},\lambda}^2}{c^2} \bar{\epsilon}_r(\mathbf{q}, z, \omega_\lambda) \mathbf{A}_{\mathbf{q},\lambda}(z), \quad (49)$$

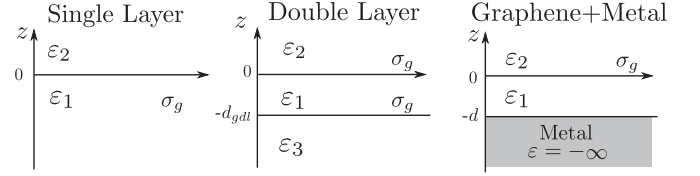


FIG. 1. Schematic representation of the three systems considered in this paper: a single graphene layer (left), a graphene double layer (center), and a graphene sheet near a perfect metal. The quantities ϵ_n refer to the dielectric permittivity of the medium n and σ_g refers to the optical conductivity of graphene.

where $\bar{\epsilon}_r(\mathbf{q}, z, \omega)$ is the dielectric function including graphene, Eq. (40),

$$\bar{\epsilon}_r(\mathbf{q}, z, \omega_\lambda) = \bar{\epsilon}_d(z) + \sum_{\ell} i \frac{\bar{\sigma}_{g\ell}(\mathbf{q}, \omega)}{\epsilon_0 \omega} \delta(z - z_\ell), \quad (50)$$

where $\bar{\epsilon}_d(z)$ is the dielectric constant of the medium, which we assume to be isotropic and a piecewise homogeneous function of z , and ℓ labels the graphene layers which are located at the planes $z = z_\ell$, with conductivity $\bar{\sigma}_{g\ell}(\mathbf{q}, \omega)$. The presence of the δ functions in Eq. (50) implies boundary conditions at each interface located at $z = z_\ell$:

$$\hat{\mathbf{z}} \times [\mathbf{E}_{\mathbf{q},\lambda}(z_\ell^+) - \mathbf{E}_{\mathbf{q},\lambda}(z_\ell^-)] = 0, \quad (51)$$

$$\hat{\mathbf{z}} \times [\mathbf{B}_{\mathbf{q},\lambda}(z_\ell^+) - \mathbf{B}_{\mathbf{q},\lambda}(z_\ell^-)] = \mu_0 \mathbf{J}_{s,\mathbf{q},\lambda}(z_\ell), \quad (52)$$

where $\mathbf{E}_{\mathbf{q},\lambda}(z) = i\omega_{\mathbf{q},\lambda} \mathbf{A}_{\mathbf{q},\lambda}(z)$ and $\mathbf{B}_{\mathbf{q},\lambda}(z) = D_{\mathbf{q}} \times \mathbf{A}_{\mathbf{q},\lambda}(z)$ are the electric and magnetic fields corresponding to mode $\mathbf{A}_{\mathbf{q},\lambda}(z)$, and $\mathbf{J}_{s,\mathbf{q},\lambda}(z_\ell) = \bar{\sigma}_{g\ell}(\mathbf{q}, \omega) \cdot \mathbf{E}_{\mathbf{q},\lambda}(z_\ell)$ is the surface current in the graphene layer ℓ . In addition to the boundary conditions (51) and (52), to determine the plasmon modes one must impose that the fields decay for $z \rightarrow \pm\infty$. Having determined the plasmon mode function, $\mathbf{A}_{\mathbf{q},\text{sp}}(z)$, and dispersion, $\omega_{\mathbf{q},\text{sp}}$, the mode normalization constant can be obtained from Eqs. (47) and (50) as

$$N_{\mathbf{q},\text{sp}} = \int dz \epsilon_d(z) \mathbf{A}_{\mathbf{q},\text{sp}}^*(z) \cdot \mathbf{A}_{\mathbf{q},\text{sp}}(z) + \frac{i}{2\epsilon_0\omega_{\mathbf{q},\lambda}} \times \sum_{\ell} \mathbf{A}_{\mathbf{q},\text{sp}}^*(z_\ell) \cdot \frac{\partial}{\partial \omega} [\omega \bar{\sigma}_{g\ell}(\mathbf{q}, \omega)]_{\omega=\omega_{\mathbf{q},\text{sp}}} \cdot \mathbf{A}_{\mathbf{q},\text{sp}}(z_\ell). \quad (53)$$

We will now analyze the different structures in detail.

A. Single layer graphene

We first discuss the simplest case of a single graphene sheet (see left panel of Fig. 1). The problem of finding the spectrum of the surface plasmons in a graphene sheet was first considered in [53] and a detailed derivation can be found in Refs. [54,55]. We assume that the single layer of graphene is located at $z = 0$, with an encapsulating dielectric medium $n = 2$ for $z > 0$ and a medium $n = 1$ for $z < 0$, such that

$$\epsilon_d(z) = \begin{cases} \epsilon_2, & z > 0, \\ \epsilon_1, & z < 0. \end{cases} \quad (54)$$

In order to determine the plasmon mode, we look for p -polarized solutions of the electric field (the electric field lies

in the plane of incidence) in the form of evanescent waves for $z \rightarrow \pm\infty$. In each piecewise homogeneous region we have that $D_{\mathbf{q}} \cdot \mathbf{E}_{\mathbf{q},\lambda}(z) = 0$. The mode function must then take the form

$$\mathbf{A}_{\mathbf{q},\text{sp}}(z) = \begin{cases} A_2^+ \mathbf{u}_{2,\mathbf{q}}^+ e^{-\kappa_{2,\mathbf{q}} z}, & z > 0, \\ A_1^- \mathbf{u}_{1,\mathbf{q}}^- e^{\kappa_{1,\mathbf{q}} z}, & z < 0, \end{cases} \quad (55)$$

where

$$\kappa_{n,\mathbf{q}} = \sqrt{q^2 - \frac{\omega_{\mathbf{q},\text{sp}}^2}{c_n^2}}, \quad (56)$$

with $c_n = c/\sqrt{\epsilon_n}$ the speed of light in medium n , and we introduced the vectors

$$\mathbf{u}_{n,\mathbf{q}}^\pm = i \frac{\mathbf{q}}{q} \mp \frac{q}{\kappa_{n,\mathbf{q}}} \hat{\mathbf{z}}. \quad (57)$$

Imposing the boundary conditions (51) and (52), we obtain the following implicit relation for the surface plasmon dispersion:

$$\frac{\epsilon_1}{\kappa_{1,\mathbf{q}}} + \frac{\epsilon_2}{\kappa_{2,\mathbf{q}}} + i \frac{\sigma_g(\mathbf{q}, \omega_{\mathbf{q},\text{sp}})}{\epsilon_0 \omega_{\mathbf{q},\text{sp}}} = 0. \quad (58)$$

In general, Eq. (58) has no analytical solution, except in the simple case where $\epsilon_1 = \epsilon_2 = \epsilon$, whose solution reduces to solving a quadratic equation. In this case, and including the effect of the degeneracy pressure, the surface plasmon-polariton dispersion relation becomes

$$\omega_{\mathbf{q},\text{sp}}^2 = \frac{1}{2} \frac{D}{2\epsilon_0 \epsilon} \sqrt{4q^2 + \left(\frac{D}{2\epsilon_0 c^2}\right)^2 - \frac{4\beta^2 q^2 \epsilon}{c^2}} - \frac{1}{2} \left(\frac{D}{2\epsilon_0 \sqrt{\epsilon} c}\right)^2 + \beta^2 q^2. \quad (59)$$

In the electrostatic limit, $c \rightarrow \infty$, the dispersion relation can also be obtained in the case when $\epsilon_1 \neq \epsilon_2$ [43]:

$$\omega_{\mathbf{q},\text{sp}}^2 = \frac{D}{\epsilon_0(\epsilon_1 + \epsilon_2)} q + \beta^2 q^2. \quad (60)$$

Thus, for the same frequency, the inclusion of the degeneracy pressure increases the surface plasmon-polariton wavelength, reducing q , $\kappa_{n,\mathbf{q}}$ and, consequently, reducing the confinement in the out-of-plane direction, making the plasmon polariton more susceptible to the external dielectric profile.

The corresponding mode function can be written as

$$\mathbf{A}_{\mathbf{q},\text{sp}}(z) = \begin{cases} \mathbf{u}_{2,\mathbf{q}}^+ e^{-\kappa_{2,\mathbf{q}} z}, & z > 0, \\ \mathbf{u}_{1,\mathbf{q}}^- e^{\kappa_{1,\mathbf{q}} z}, & z < 0, \end{cases} \quad (61)$$

and the mode normalization constant is obtained according to Eq. (53) as

$$N_{\mathbf{q},\text{sp}} = \frac{\epsilon_2}{2\kappa_{2,\mathbf{q}}^3} (\kappa_{2,\mathbf{q}}^2 + q^2) + \frac{\epsilon_1}{2\kappa_{1,\mathbf{q}}^3} (\kappa_{1,\mathbf{q}}^2 + q^2) + \frac{D}{\epsilon_0} \frac{\beta^2 q^2}{(\omega^2 - \beta^2 q^2)^2}, \quad (62)$$

where the last term is due to the dispersion in the graphene layer. We point out that, within the hydrodynamic model used for conductivity of graphene, this contribution is only nonzero if nonlocal effects are also included, that is, if $\beta \neq 0$.

B. Graphene-metal structure

We now move to the more complex case of a graphene sheet near a perfect metal (see right panel of Fig. 1). We assume that the metal interface is located at $z = -d$ and the graphene layer is located at $z = 0$. The dielectric constant is given by

$$\epsilon_d(z) = \begin{cases} \epsilon_2, & z > 0, \\ \epsilon_1, & 0 > z > -d. \end{cases} \quad (63)$$

Noticing that the plasmon field should decay for $z \rightarrow \infty$, the mode function should have the form

$$\mathbf{A}_{\mathbf{q},\text{sp}}(z) = \begin{cases} A_2^+ \mathbf{u}_{2,\mathbf{q}}^+ e^{-\kappa_{2,\mathbf{q}} z}, & z > 0, \\ A_1^+ \mathbf{u}_{1,\mathbf{q}}^+ e^{-\kappa_{1,\mathbf{q}} z} + A_1^- \mathbf{u}_{1,\mathbf{q}}^- e^{\kappa_{1,\mathbf{q}} z}, & 0 > z > -d. \end{cases} \quad (64)$$

Notice that the presence of a perfect metal at $z = -d$ implies that the tangential component of the electric field should vanish. Imposing the previous condition and the boundary conditions (51) and (52) at $z = 0$, we obtain a homogeneous system of equations

$$\begin{bmatrix} 1 & -1 & -1 \\ \xi_{2,\mathbf{q}} & -\frac{\epsilon_1}{\kappa_{1,\mathbf{q}}} & \frac{\epsilon_1}{\kappa_{1,\mathbf{q}}} \\ 0 & e^{\kappa_{1,\mathbf{q}} d} & e^{-\kappa_{1,\mathbf{q}} d} \end{bmatrix} \begin{bmatrix} A_2^+ \\ A_1^+ \\ A_1^- \end{bmatrix} = 0, \quad (65)$$

where $\xi_{2,\mathbf{q}} = \frac{\epsilon_2}{\kappa_{2,\mathbf{q}}} + i \frac{\sigma_g L}{\epsilon_0 \omega}$. The dispersion relation of the screened plasmons is obtained by looking for the zero of the determinant of the previous matrix, which leads to the condition for the dispersion relation

$$\frac{\epsilon_1}{\kappa_{1,\mathbf{q}}} \coth(\kappa_{1,\mathbf{q}} d) + \frac{\epsilon_2}{\kappa_{2,\mathbf{q}}} + i \frac{\sigma_g}{\omega \epsilon_0} = 0. \quad (66)$$

The boundary conditions imply that the mode function is given by

$$\mathbf{A}_{\mathbf{q},\text{sp}}(z) = \begin{cases} \sinh(\kappa_{1,\mathbf{q}} d) \mathbf{u}_{2,\mathbf{q}}^+ e^{-\kappa_{2,\mathbf{q}} z}, & z > 0, \\ i \frac{\mathbf{q}}{q} \sinh[\kappa_{1,\mathbf{q}}(z+d)] \\ + \frac{q}{\kappa_{1,\mathbf{q}}} \hat{\mathbf{z}} \cosh[\kappa_{1,\mathbf{q}}(z+d)], & 0 > z > -d. \end{cases} \quad (67)$$

The mode normalization constant can be determined from Eq. (53), and we obtain

$$N_{\mathbf{q},\text{sp}} = \frac{\epsilon_2}{2\kappa_{2,\mathbf{q}}^3} \sinh^2(\kappa_{1,\mathbf{q}} d) (\kappa_{2,\mathbf{q}}^2 + q^2) + \frac{\epsilon_1}{2\kappa_{1,\mathbf{q}}^3} \left[\frac{1}{2} \sinh(2\kappa_{1,\mathbf{q}} d) (\kappa_{1,\mathbf{q}}^2 + q^2) + d \kappa_{1,\mathbf{q}} \epsilon_1 \frac{\omega^2}{c^2} \right] + \sinh^2(\kappa_{1,\mathbf{q}} d) \frac{D}{\epsilon_0} \frac{\beta^2 q^2}{(\omega^2 - \beta^2 q^2)^2}, \quad (68)$$

where, as in Eq. (62), the last term is due to the dispersion of graphene.

We note that the dispersion relation for the screened plasmons, Eq. (66), is the same one that would be obtained for the acoustic plasmons in a symmetric graphene double layer structure (center panel of Fig. 1). In this structure, we have two graphene layers located at $z = 0$ and $z = -d_{\text{gdL}}$. The dielectric

constant of the encapsulating medium is given by

$$\epsilon_d(z) = \begin{cases} \epsilon_2, & z > 0, \\ \epsilon_1, & 0 > z > -d_{\text{gdl}}, \\ \epsilon_3, & -d_{\text{gdl}} > z. \end{cases} \quad (69)$$

Since the plasmonic modes should decay for $z \rightarrow \pm\infty$, the plasmon mode function must have the form

$$\mathbf{A}_{\mathbf{q},\text{sp}}(z) = \begin{cases} A_2^+ \mathbf{u}_{2,\mathbf{q}}^+ e^{-\kappa_2 \mathbf{q} z}, & z > 0, \\ A_1^+ \mathbf{u}_{1,\mathbf{q}}^+ e^{-\kappa_1 \mathbf{q} z} + A_1^- \mathbf{u}_{1,\mathbf{q}}^- e^{\kappa_1 \mathbf{q} z}, & 0 > z > -d_{\text{gdl}}, \\ A_3^- \mathbf{u}_{3,\mathbf{q}}^- e^{\kappa_3 \mathbf{q} z}, & -d_{\text{gdl}} > z. \end{cases} \quad (70)$$

Imposing the boundary conditions (51) and (52) at $z = 0$ and $z = -d_{\text{gdl}}$, we obtain the following homogeneous system of equations:

$$\begin{bmatrix} 1 & -1 & -1 & 0 \\ \xi_{2,\mathbf{q}} & -\frac{\epsilon_1}{\kappa_{1,\mathbf{q}}} & \frac{\epsilon_1}{\kappa_{1,\mathbf{q}}} & 0 \\ 0 & e^{\kappa_{1,\mathbf{q}} d_{\text{gdl}}} & e^{-\kappa_{1,\mathbf{q}} d_{\text{gdl}}} & -e^{-\kappa_{3,\mathbf{q}} d_{\text{gdl}}} \\ 0 & \frac{\epsilon_1}{\kappa_{1,\mathbf{q}}} e^{\kappa_{1,\mathbf{q}} d_{\text{gdl}}} & -\frac{\epsilon_1}{\kappa_{1,\mathbf{q}}} e^{-\kappa_{1,\mathbf{q}} d_{\text{gdl}}} & \xi_{3,\mathbf{q}} e^{-\kappa_{3,\mathbf{q}} d_{\text{gdl}}} \end{bmatrix} \begin{bmatrix} A_2^+ \\ A_1^+ \\ A_1^- \\ A_3^- \end{bmatrix} = 0, \quad (71)$$

where $\xi_{2,\mathbf{q}} = \frac{\epsilon_2}{\kappa_{2,\mathbf{q}}} + i \frac{\sigma_{\text{gtop},L}}{\epsilon_0 \omega}$ and $\xi_{3,\mathbf{q}} = \frac{\epsilon_3}{\kappa_{3,\mathbf{q}}} + i \frac{\sigma_{\text{gbot},L}}{\epsilon_0 \omega}$. The dispersion relation is obtained by finding the zeros of the determinant of the previous matrix. Since the system is composed of two graphene sheets the double layer structure has two dispersion branches, a low energy one—the acoustic mode—and a high energy one—the optical mode. In the optical mode, the charge oscillations in the two graphene sheets are in phase, whereas, in the acoustic mode, the charge oscillations are out of phase. In the particular case of a symmetric structure, with $\epsilon_2 = \epsilon_3$ and equal conductivities for the top and bottom graphene layers, $\sigma_{\text{gtop},L} = \sigma_{\text{gbot},L} = \sigma_{g,L}$, the determinant factorizes, yielding two independent expressions:

$$\frac{\epsilon_1}{\kappa_1} \tanh\left(\frac{\kappa_1 d_{\text{gdl}}}{2}\right) + \frac{\epsilon_2}{\kappa_2} + i \frac{\sigma_{g,L}}{\omega \epsilon_0} = 0 \quad (72)$$

for the optical mode and

$$\frac{\epsilon_1}{\kappa_1} \coth\left(\frac{\kappa_1 d_{\text{gdl}}}{2}\right) + \frac{\epsilon_2}{\kappa_2} + i \frac{\sigma_{g,L}}{\omega \epsilon_0} = 0 \quad (73)$$

for the acoustic one. Notice that Eq. (73) for the acoustic mode dispersion coincides with Eq. (66) for the screened plasmon, provided $d_{\text{gdl}} = 2d$. This fact can be understood in terms of image charges as illustrated in Fig. 2.

An alternative way to obtain the plasmon dispersion relation is to look for poles (or resonances in the presence of losses) in the so-called loss function [55], which is defined as

$$\mathcal{L}(\mathbf{q}, \omega) = -\text{Im}[r_p(\mathbf{q}, \omega)], \quad (74)$$

where $r_p(\mathbf{q}, \omega)$ is the reflection coefficient of the structure in consideration for the p polarization, and \mathbf{q} and ω are, respectively, the in-plane wave vector and frequency of the impinging radiation (see Appendix B). For a symmetric graphene double layer ($\epsilon_2 = \epsilon_3$ and $\sigma_{\text{gtop},L} = \sigma_{\text{gbot},L}$), this coefficient has poles at the solutions of Eqs. (72) and (73), as can be seen comparing those equations with Eq. (B5). The loss function for the double layer graphene is depicted in the top panel of

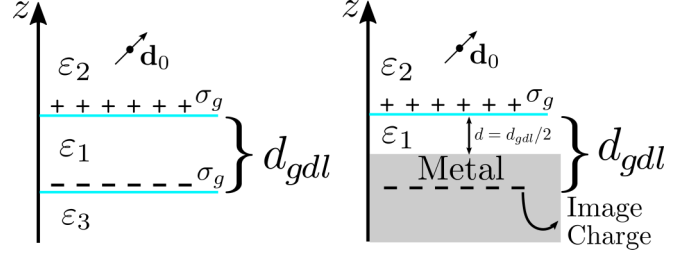


FIG. 2. Comparison of the double layer graphene system and the graphene-metal case. Due to the image charges in the graphene-metal structure, the spectrum of a symmetric ($\epsilon_2 = \epsilon_3$ and $\sigma_{\text{gtop},L} = \sigma_{\text{gbot},L}$) double layer graphene is equivalent to that of the graphene-metal system if we take into account that graphene is at a distance $d = d_{\text{gdl}}/2$ from the metal, where d_{gdl} is the interlayer distance in the double layer case.

Fig. 3, as function of ω and of the dimensionless parameter $s = qc/\omega$, which defines the dispersion relation of the single graphene layer, clad by two different dielectrics of dielectric functions ϵ_1 and ϵ_2 , in the electrostatic limit by

$$\omega(s) = \frac{4\alpha E_F}{\epsilon_1 + \epsilon_2} s, \quad (75)$$

where E_F is the Fermi energy of graphene and α is the fine structure constant of vacuum. In the top panel of Fig. 3 two branches are clearly seen: a high energy one—the optical branch—and the acoustic branch at lower energies. At high energies and high s the two branches merge and converge to the single layer branch. The reader may wonder why the lower branch starts at finite momentum. This happens due to the definition of the s parameter, which involves both the frequency and the real wave number q . This choice allows one to clearly separate the two branches in the (ω, s) plane. In the bottom panel of Fig. 3 we depict the loss function for the graphene-metal system. Clearly, only one branch is seen, which coincides with the acoustic branch of the double layer graphene upon considering d equal to half that of the double layer system, as explained in Fig. 2.

V. APPLICATION: QUANTUM EMISSION CLOSE TO GRAPHENE STRUCTURES

We will now apply the quantization of the plasmon modes in graphene structures to the problem of spontaneous emission by a quantum emitter which is located above the structure. We model the quantum emitter as a two-level system embedded in medium 2 at position $\mathbf{r}_0 = (0, 0, z_0)$. The quantum emitter couples to the plasmonic field via dipolar coupling: $\hat{H}_{\text{sp-d}} = -\hat{\mathbf{d}} \cdot \hat{\mathbf{E}}_{\text{sp}}(\mathbf{r}_0)$, with

$$\hat{\mathbf{E}}_{\text{sp}}(\mathbf{r}) = \sum_{\mathbf{q}} i \sqrt{\frac{\hbar \omega_{\mathbf{q},\text{sp}}}{2S \epsilon_0 N_{\mathbf{q},\text{sp}}}} \mathbf{A}_{\mathbf{q},\text{sp}}(z) e^{i\mathbf{q} \cdot \mathbf{x}} \hat{a}_{\mathbf{q},\text{sp}} + \text{H.c.}, \quad (76)$$

the plasmon mode electric-field operator, and $\hat{\mathbf{d}} = \mathbf{d}_{ge} \hat{c}_g^\dagger \hat{c}_e + \text{H.c.}$, the emitter dipole operator, where $\hat{c}_{g/e}^\dagger$ ($\hat{c}_{g/e}$) is the creation (annihilation) operator for the ground (g) and excited (e) state of the two-level system and $\mathbf{d}_{ge} = \langle g | \hat{\mathbf{d}} | e \rangle$ is the dipole matrix element.

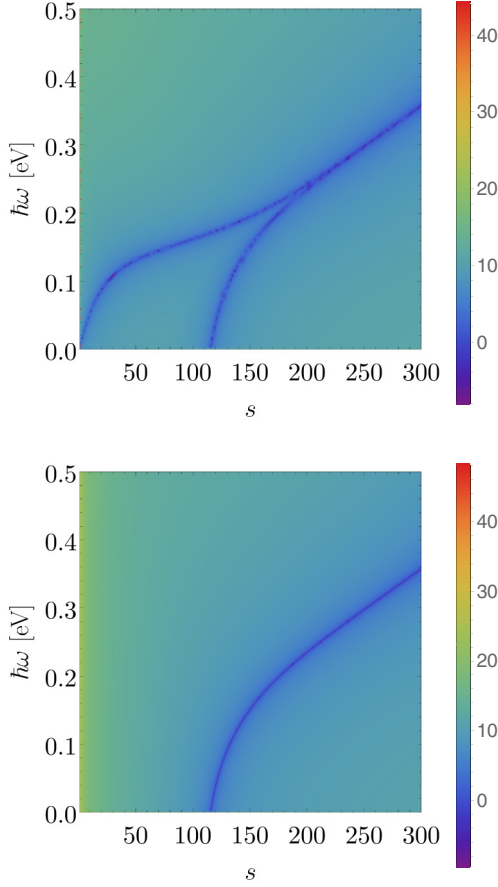


FIG. 3. Loss function [Eq. (74)] for the p -polarization reflection coefficient for (top panel) a graphene double layer structure and (bottom panel) graphene near a perfect metal. The parameters used in the top panel are $d_{\text{gdl}} = 20$ nm, $\epsilon_3 = 1$, and for the bottom panel $d = 10$ nm. The remaining parameters used in both panels are $\epsilon_1 = 3.9$, $\epsilon_2 = 1$, and $E_F = 0.2$ eV. In both plots, nonlocal effects were neglected ($\beta = 0$) and a lossy graphene conductivity with a broadening of $\hbar\gamma = 10$ meV (see Appendix C) was used.

The transition rate of an emitter due to the emission of graphene surface plasmons is given by Fermi's golden rule [56,57]:

$$\Gamma_{\text{sp}} = \frac{2\pi}{\hbar} \sum_{\mathbf{q}} |\langle g; n_{\mathbf{q},\text{sp}} + 1 | \hat{\mathbf{d}} \cdot \hat{\mathbf{E}} | e; n_{\mathbf{q},\text{sp}} \rangle|^2 \delta(\hbar\omega_0 - \hbar\omega_{\mathbf{q},\text{sp}}), \quad (77)$$

where ω_0 is the transition frequency, $|e; n_{\mathbf{q},\text{sp}}\rangle$ represents the initial state with $n_{\mathbf{q},\text{sp}}$ plasmons in graphene and the emitter in the excited state, and $|g; n_{\mathbf{q},\text{sp}} + 1\rangle$ represents the final state with one more graphene surface plasmon and the emitter in the ground state. The transition matrix element for spontaneous plasmon emission, when there are no surface plasmons in the initial state, is given by

$$\langle g; 1 | \hat{\mathbf{d}} \cdot \hat{\mathbf{E}} | e; 0 \rangle = -i \sqrt{\frac{\hbar\omega_{\mathbf{q},\text{sp}}}{2S\epsilon_0 N_{\mathbf{q},\text{sp}}}} \mathbf{d}_{ge} \cdot \mathbf{A}_{\mathbf{q},\text{sp}}^*(z_0). \quad (78)$$

With this result the transition rate reads

$$\Gamma_{\text{sp}} = \frac{1}{4\pi\hbar\epsilon_0} \int d^2\mathbf{q} \frac{\hbar\omega_{\mathbf{q},\text{sp}}}{N_{\mathbf{q},\text{sp}}} |\mathbf{d}_{ge} \cdot \mathbf{A}_{\mathbf{q},\text{sp}}^*(z_0)|^2 \delta(\hbar\omega_0 - \hbar\omega_{\mathbf{q},\text{sp}}). \quad (79)$$

Using the mode function we can write

$$|\mathbf{d}_{ge} \cdot \mathbf{A}_{\mathbf{q},\text{sp}}^*(z_0)|^2 = \mathcal{G}_{\mathbf{q}} |\mathbf{d}_{ge}|^2 e^{-2\kappa_{2,\mathbf{q}}z_0} \times \left(\cos^2\phi \sin^2\psi + \frac{q^2}{\kappa_{2,\mathbf{q}}^2} \cos^2\psi \right), \quad (80)$$

where ψ is the angle that the dipole makes with the axis perpendicular to graphene (z axis) and ϕ is the azimuthal angle. The prefactor $\mathcal{G}_{\mathbf{q}}$ is defined as $\mathcal{G}_{\mathbf{q}} = 1$ for the single-layer graphene case and as $\mathcal{G}_{\mathbf{q}} = \sinh^2(\kappa_{1,\mathbf{q}}d)$ for the graphene + metal structure. Using the in-plane isotropy of the system, the momentum integration in Eq. (79) can be trivially performed, yielding

$$\Gamma_{\text{sp}} = \mathcal{G}_{\mathbf{q}_0} \frac{q_0\omega_{\mathbf{q}_0,\text{sp}}}{N_{\mathbf{q}_0,\text{sp}}} \left(\frac{\partial\omega_{\mathbf{q}_0,\text{sp}}}{\partial q} \right)^{-1} \frac{|\mathbf{d}_{ge}|^2}{4\hbar\epsilon_0} e^{-2\kappa_{2,\mathbf{q}_0}z_0} \times \left(\sin^2\psi + 2\frac{q^2}{\kappa_{2,\mathbf{q}_0}^2} \cos^2\psi \right), \quad (81)$$

where q_0 is the momentum of a surface plasmon, with frequency ω_0 , i.e., $\omega_0 = \omega_{\mathbf{q}_0,\text{sp}}$. So far the expression for Γ_{sp} is general. The differences arise from the particular forms of the dispersion $\omega_{\mathbf{q},\text{sp}}$, the mode normalization constant $N_{\mathbf{q},\text{sp}}$, and the prefactor $\mathcal{G}_{\mathbf{q}}$.

A. Decay rate for local conductivity

We will now study the plasmon emission rate, when non-local effects are neglected, $\beta = 0$ in Eq. (38).

We first focus on the case of a quantum emitter close to a single graphene layer and the same dielectric above and below the graphene layer, $\epsilon_1 = \epsilon_2 = \epsilon$. Using the analytic solution of Eq. (58) for this case, we can write Eq. (81) as

$$\Gamma_{\text{sp}}^{\text{gsl}} = \frac{d_{ge}^2}{4\hbar\epsilon_0} \left[2\omega_0^4 \left(\frac{\hbar}{2\alpha E_F c} \right)^2 + \frac{\omega_0^2 \epsilon}{c^2} \right] \frac{e^{-2\kappa_{\mathbf{q}_0}z_0}}{N_{\mathbf{q}_0,\text{sp}}} \times \left\{ \sin^2\psi + \frac{2}{\kappa_{\mathbf{q}_0}^2} \left[\omega_0^4 \left(\frac{\hbar}{2\alpha E_F c} \right)^2 + \frac{\omega_0^2 \epsilon}{c^2} \right] \cos^2\psi \right\}. \quad (82)$$

In Figs. 4 and 5, we plot the ratio $\Gamma_{\text{sp}}^{\text{gsl}}/\Gamma_0$, where $\Gamma_0 = d_{ge}^2\omega_0^3/(3\pi\epsilon_0\hbar c^3)$ is the total decay rate of an emitter in vacuum, for different graphene-quantum emitter distances z_0 and dipole orientations. For comparison, we also display the ratio $\Gamma_{\text{full}}/\Gamma_0$, where Γ_{full} is the total decay rate of the quantum emitter (which includes decay due to emission of plasmons and free radiation, and also decay due to Ohmic losses in the conductivity of graphene, as introduced in Appendix C).

The total decay rate can be computed from the knowledge of the reflection coefficients, which are incorporated into the dyadic EM Green's function [55,56,58] (see Ref. [59] for a detailed study of the properties of an emitter near graphene

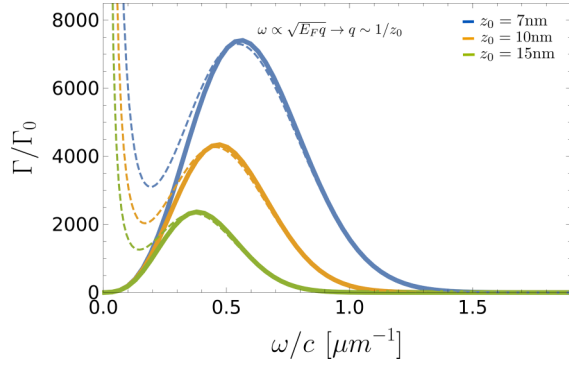


FIG. 4. Decay rate of a quantum emitter close to a single graphene layer as a function of emitter frequency, for different emitter-graphene distances z_0 . The solid lines show the decay rate due to plasmon emission as evaluated with Eq. (82). The dashed lines show the total decay rate computed using Eq. (83). The parameters used are $\epsilon_1 = \epsilon_2 = 1$, $E_F = 0.3$ eV, and $\cos^2 \psi = 1/3$. For the evaluation of the total decay rate a broadening of $\hbar\gamma = 4$ meV was used in the conductivity of graphene (see Appendix C). The local form of graphene conductivity was used ($\beta = 0$).

using dyadic Green's functions). For a dipole in medium $n = 2$, the total decay rate is given by

$$\begin{aligned} \frac{\Gamma_{\text{full}}}{\Gamma_0} \epsilon_2 \left(\frac{c_2}{c}\right)^3 &= 1 + \frac{3}{2} \cos^2 \psi \operatorname{Re} \int \frac{dk}{k_2^3} \frac{k^3}{k_{z,2}} r_p e^{i2k_{z,2}z_0} \\ &+ \frac{3}{4} \sin^2 \psi \operatorname{Re} \int \frac{dk}{k_2} \frac{k}{k_{z,2}} \left(r_s - \frac{k_{z,2}^2}{k_2^2} r_p \right) \\ &\times e^{i2k_{z,2}z_0}, \end{aligned} \quad (83)$$

where $r_{s/p}$ are reflection coefficients for the s/p polarization; $k_n = \omega/c_n$ and $k_{z,n}$ are defined in Appendix B. The conduc-

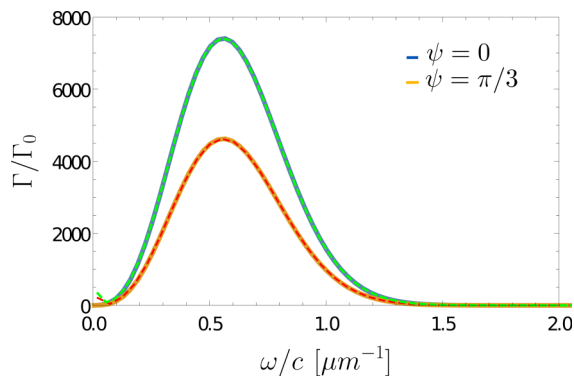


FIG. 5. Decay rate of a quantum emitter close to a single graphene layer as a function of emitter frequency, for different dipole orientations: $\psi = 0$ and $\psi = \pi/3$. Solid lines show the plasmon emission rate [Eq. (82)] and the dashed lines show the total decay rate [Eq. (83)]. The parameters considered were $z_0 = 70$ nm, $E_F = 0.4$ eV, and $\epsilon_1 = \epsilon_2 = 1$. In the evaluation of the total decay rate a broadening factor of $\hbar\gamma = 0.1$ meV was used in the conductivity of graphene (see Appendix C). For such small Ohmic losses, the decay rate is completely dominated by the plasmon emission. The local form of graphene conductivity was used ($\beta = 0$).

tivity of graphene, including Ohmic losses, is encoded in the reflection coefficients and is given in Appendix C.

A number of details are worth mentioning. There are two distinct behaviors of the decay rate Γ_{full} . At low frequency the curves shoot up due to Ohmic losses, which are not included in Eq. (82), which only takes into account emission of well defined plasmons. At intermediate frequencies, the curves develop a clear resonance due to the excitation of surface plasmons in graphene. Also the maximum of the resonances blueshifts with the decrease of the distance of the dipole to the graphene sheet. This behavior is easily explained remembering that the dispersion of the surface plasmons in single layer graphene is proportional to \sqrt{q} . Since the distance z_0 introduces a momentum scale $q \sim 1/z_0$, smaller z_0 values correspond to higher q values and higher energies of the resonant maximum. Equation (82) for the plasmon emission rate produces exactly the same resonance (same magnitude and same maximum of the resonance position) as Γ_{full} , indicating that, in this region, the decay rate of the quantum emitter is dominated by plasmon emission. This is further shown in Fig. 5, where losses were arbitrarily reduced in the evaluation of Γ_{full} . We can also avoid the superposition of the Ohmic and surface plasmon contributions choosing either a larger Fermi energy or a larger distance from graphene to the metal. In Fig. 5 the ratio Γ/Γ_0 is smaller than the ones in Fig. 4 due to the larger distance of the dipole to the graphene sheet.

An analytic expression for the plasmon emission rate can be also obtained for the case of graphene-metal structure assuming that $\kappa_{1,q_0}d \ll 1$. In this limit, Eq. (66) can be approximately solved, yielding $\hbar\omega_{q,\text{sp}} = \sqrt{4\alpha d E_F \hbar c / \epsilon} q$. Plugging this result in Eq. (81), we obtain

$$\begin{aligned} \Gamma_{\text{sp}}^{\text{gm}} &\simeq \frac{d_{12}^2}{4\epsilon_0 \hbar} \frac{\epsilon \sinh^2(\kappa_{1,q_0}d)}{4\alpha d E_F \hbar c} \frac{(\hbar\omega)^2 e^{-2\kappa_{2,q_0}z_0}}{N_{q_0,\text{sp}}} \\ &\times \left(\sin^2 \psi + 2 \frac{q^2}{\kappa_{2,q_0}^2} \cos^2 \psi \right). \end{aligned} \quad (84)$$

This plasmon emission rate is shown in Fig. 6 as a function of the emitter frequency, ω , and the graphene-metal separation d . As in the case of a single graphene layer, for each d there is a well defined peak as function of ω .

B. Decay rate with nonlocal effects

We now focus on the role that nonlocal effects in graphene's conductivity play in the emitter decay rate. We will restrict ourselves to the case of a quantum emitter close to a single layer of graphene. From the results of Sec. IV A, we expect that the inclusion of nonlocal effects (finite β) will result in a smaller momentum q . Since the in-plane momentum q also controls the extension of the plasmon mode function away from the graphene layer, a smaller q would lead to a more extended (deconfined) plasmon, which in principle would couple more efficiently to a quantum emitter placed away from the graphene layer, leading to an increase of the quantum emitter decay rate. On the other hand, as it can also be seen from Eq. (60), the inclusion of nonlocal effects leads to a linearization of the surface plasmon-polariton dispersion

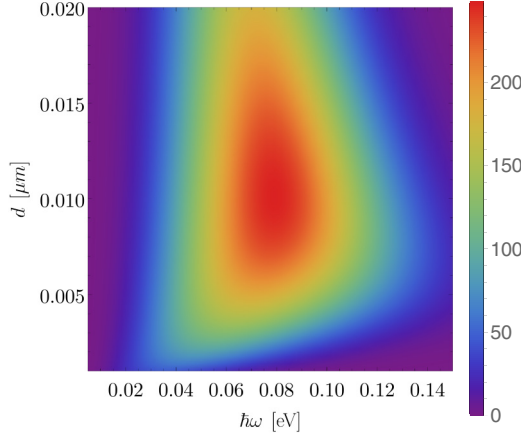


FIG. 6. Density plot of the transition rate of a quantum emitter due to the emission of surface plasmons in a graphene-metal structure, as given by Eq. (84). The used parameters are $z_0 = 30$ nm, $E_F = 0.2$ eV, $\epsilon_1 = 3.9$, and $\epsilon_2 = 1$, $\psi = 0$. Making line cuts at constant d we can easily see the presence of a resonance in the dipole transition rate due to the excitation of graphene screened plasmons.

relation and, consequently, to a reduction in the plasmonic density of states, which would contribute to a reduction of the emitter decay rate.

For a single layer of graphene when $\epsilon_1 = \epsilon_2 = \epsilon$, it is possible to obtain an analytic expression for the decay rate due to plasmons, including effects of nonlocality and retardation. The dispersion relation Eq. (59) can be inverted to express the plasmon momentum, q_0 , as a function of its frequency, ω_0 . The obtained expression is given by

$$q_0^2 = \left(\frac{\sqrt{\left(\frac{D}{2\epsilon_0\epsilon}\right)^2 + 4\beta^2\omega_0^2} - 4\beta^4\frac{\epsilon\omega_0^2}{c^2} - \left(\frac{D}{2\epsilon_0\epsilon}\right)}{2\beta^2} \right)^2 + \frac{\epsilon\omega_0^2}{c^2}. \quad (85)$$

This result together with the fact that, from Eq. (60),

$$\frac{\partial\omega_{q_0,sp}}{\partial q} = \frac{1}{\omega} \frac{\frac{D}{2\epsilon_0\epsilon} \frac{q_0}{\kappa_{q_0}} + 2\beta^2 q_0}{2 + \frac{D}{2\epsilon_0\epsilon} \frac{1}{c^2} \frac{\epsilon}{\kappa_{q_0}}} \quad (86)$$

allows us to use Eq. (81) to express the decay rate of a quantum emitter analytically. In Fig. 7, we compare the transition rate of a quantum emitter calculated taking into account nonlocal effects in the optical response of graphene, $\beta \neq 0$ in Eq. (38), with the local case, $\beta = 0$. We can see that the nonlocal effects contribute to a reduction in the decay rate of the emitter, showing that the reduction in the plasmonic density of states is a more important effect than the reduction in the confinement of the graphene plasmon. Furthermore, nonlocal effects play a more important role for smaller emitter-graphene distances. This can be understood if we analyze the electrostatic limit, $c \rightarrow \infty$, of the decay rate, which is also shown in Fig. 7. Within the electrostatic approximation, it is possible to find an analytic expression for the decay rate even if $\epsilon_1 \neq \epsilon_2$. The obtained result can be

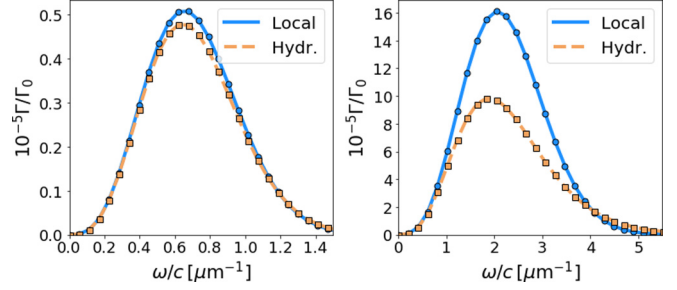


FIG. 7. Comparison between the plasmon emission rate of a quantum emitter close to a single layer of graphene using the local ($\beta = 0$) and nonlocal (hydr.) ($\beta \neq 0$) models for the graphene conductivity [see Eq. (38)]. The circle and square markers show the results obtained taking into account retardation effects for the local and nonlocal cases, respectively. The solid and dashed lines show the corresponding results within the electrostatic approximation, according to Eq. (87). The used parameters are $E_F = 0.6$ eV, $\epsilon_1 = \epsilon_2 = 3.9$, and $\psi = 0$. Left panel: $z_0 = 20$ nm. Right panel: $z_0 = 2$ nm. The nonlocal effects lead to a decrease in resonance in the transition rate. This effect is more pronounced for small values of the separation z_0 between the quantum emitter and the graphene layer.

written as

$$\Gamma_{sp}^{slg} \simeq \left[\frac{1}{2} \sin^2 \psi + \cos^2 \psi \right] \frac{d_{ge}^2}{\hbar\epsilon_0(\epsilon_1 + \epsilon_2)} \frac{1}{z_0^3} \times g \left(\sqrt{\frac{\epsilon_0(\epsilon_1 + \epsilon_2)z_0}{D}} \omega, \sqrt{\frac{2\epsilon_0(\epsilon_1 + \epsilon_2)}{z_0 D}} \beta \right), \quad (87)$$

where we defined the function

$$g(y, b) = \frac{1}{\sqrt{1 + 2b^2y^2}} \left(\frac{\sqrt{1 + 2b^2y^2} - 1}{b^2} \right)^3 \times \exp \left[-2 \left(\frac{\sqrt{1 + 2b^2y^2} - 1}{b^2} \right) \right]. \quad (88)$$

As can be seen in Fig. 7, the electrostatic result is nearly indistinguishable from the result with retardation effects. The adimensional parameter $b = \sqrt{\frac{2\epsilon_0(\epsilon_1 + \epsilon_2)}{z_0 D}} \beta$ determines the relative importance of nonlocal effects, with the local case obtained when $b = 0$, in which case the function $g(y, b)$ reduces to $g(y, 0) = y^6 e^{-2y^2}$. Equations (87) and (88) make clear that, for a fixed value of β , a reduction in the separation z_0 leads to an increase in the b parameter, and therefore to an increase in importance of the nonlocal effects. Since, in graphene the Drude weight D is proportional to the Fermi energy, E_F , nonlocal effects also become more relevant at smaller doping levels.

VI. CONCLUSIONS

In this paper, we have performed the quantization of graphene plasmons, in the absence of losses, and applied the field quantization to the interaction of an emitter with doped graphene. The quantization was performed using both a macroscopic energy approach and a quantum hydrodynamic model, which allows for the inclusion of nonlocal effects in

the EM response of graphene. The employed quantization approach allows for the determination of the plasmon EM field mode functions and, importantly, their normalization, which becomes nontrivial when dispersion is included.

When comparing the total decay rate of a quantum emitter (as obtained using the full EM dyadic Green's function) with the decay rate due to plasmon quantum emission, it was shown that plasmon emission completely dominates the decay rate, for typical emitter-graphene separations and emitter frequencies. It was shown that nonlocal effects in the graphene response become increasingly important for smaller graphene-emitter separations and smaller Fermi energies.

The advantage of the quantization method developed in this work lies in its simplicity. The mode functions are obtained from the solution of the Maxwell equations for the vector potential, and the normalization of the mode functions can be expressed as a simply integral, which only involves the dielectric function of the medium. For situations when only a few modes contribute significantly to the physics, as in the case of quantum emission dominated by plasmons, mode functions allow for a much simpler and physically transparent description than the full EM dyadic Green's function. Since the determination of the mode functions only involves the solution of the classical Maxwell equations, the quantization

of the electromagnetic field of more complex structures can be easily achieved. We also note that the procedure gives the quantized form of both the electric and magnetic fields.

In possession of a quantized theory for graphene plasmons, we have set the stage for the future discussion of other quantum effects involving these collective excitations made simultaneously of light and matter.

ACKNOWLEDGMENTS

B.A.F. and N.M.R.P. acknowledge support from the European Commission through the project ‘‘Graphene-Driven Revolutions in ICT and Beyond’’ (Ref. No. 785219), and the Portuguese Foundation for Science and Technology (FCT) in the framework of the Strategic Financing UID/FIS/04650/2013. Additionally, N.M.R.P. acknowledges COMPETE2020, PORTUGAL2020, FEDER, and the Portuguese Foundation for Science and Technology (FCT) through Projects No. PTDC/FIS-NAN/3668/2013 and No. POCI-01-0145-FEDER-028114. B.A. acknowledges the hospitality of CeFEMA, where he was a visiting researcher during part of the time in which this work was developed, and financial support from Portuguese Foundation for Science and Technology (FCT) through Project No. CEECIND/02936/2017.

APPENDIX A: DIAGONALIZATION OF HYDRODYNAMIC HAMILTONIAN

1. Orthogonality of mode functions

We start by showing that the mode functions $[\mathbf{A}_{\mathbf{q},\lambda}(z), \mathbf{v}_{\mathbf{q},\lambda}]$ obey certain orthogonality conditions which will be useful. We start by writing the equations for the mode functions within the hydrodynamic model, Eqs. (33) and (34), in matrix form as

$$\begin{bmatrix} \omega_{\mathbf{q},\lambda}^2 \epsilon_0 \bar{\epsilon}_d(z) - \frac{1}{\mu_0} D_{\mathbf{q}} \times D_{\mathbf{q}} \times & i\omega_{\mathbf{q},\lambda} en_0 \delta(z) \\ -i\omega_{\mathbf{q},\lambda} en_0 \delta(z) & n_0 m (\omega_{\mathbf{q},\lambda}^2 - \beta^2 \mathbf{q} \otimes \mathbf{q}) \delta(z) \end{bmatrix} \begin{bmatrix} \mathbf{A}_{\mathbf{q},\lambda}(z) \\ \mathbf{v}_{\mathbf{q},\lambda} \end{bmatrix} = 0. \quad (\text{A1})$$

Let us now consider another mode λ' , with mode function $[\mathbf{A}_{\mathbf{q},\lambda'}(z), \mathbf{v}_{\mathbf{q},\lambda'}]$, solution of

$$\begin{bmatrix} \omega_{\mathbf{q},\lambda'}^2 \epsilon_0 \bar{\epsilon}_d(z) - \frac{1}{\mu_0} D_{\mathbf{q}} \times D_{\mathbf{q}} \times & i\omega_{\mathbf{q},\lambda'} en_0 \delta(z) \\ -i\omega_{\mathbf{q},\lambda'} en_0 \delta(z) & n_0 m (\omega_{\mathbf{q},\lambda'}^2 - \beta^2 \mathbf{q} \otimes \mathbf{q}) \delta(z) \end{bmatrix} \begin{bmatrix} \mathbf{A}_{\mathbf{q},\lambda'}(z) \\ \mathbf{v}_{\mathbf{q},\lambda'} \end{bmatrix} = 0. \quad (\text{A2})$$

Now we contract Eq. (A1) with $[\mathbf{A}_{\mathbf{q},\lambda'}^\dagger(z), \mathbf{v}_{\mathbf{q},\lambda'}^\dagger]$, Eq. (A2) with $[\mathbf{A}_{\mathbf{q},\lambda}^\dagger(z), \mathbf{v}_{\mathbf{q},\lambda}^\dagger]$, and integrate both equations over z obtaining

$$\int dz [\mathbf{A}_{\mathbf{q},\lambda'}^\dagger(z), \mathbf{v}_{\mathbf{q},\lambda'}^\dagger] \begin{bmatrix} \omega_{\mathbf{q},\lambda}^2 \epsilon_0 \bar{\epsilon}_d(z) - \frac{1}{\mu_0} D_{\mathbf{q}} \times D_{\mathbf{q}} \times & i\omega_{\mathbf{q},\lambda} en_0 \delta(z) \\ -i\omega_{\mathbf{q},\lambda} en_0 \delta(z) & n_0 m (\omega_{\mathbf{q},\lambda}^2 - \beta^2 \mathbf{q} \otimes \mathbf{q}) \delta(z) \end{bmatrix} \begin{bmatrix} \mathbf{A}_{\mathbf{q},\lambda}(z) \\ \mathbf{v}_{\mathbf{q},\lambda} \end{bmatrix} = 0, \quad (\text{A3})$$

$$\int dz [\mathbf{A}_{\mathbf{q},\lambda}^\dagger(z), \mathbf{v}_{\mathbf{q},\lambda}^\dagger] \begin{bmatrix} \omega_{\mathbf{q},\lambda'}^2 \epsilon_0 \bar{\epsilon}_d(z) - \frac{1}{\mu_0} D_{\mathbf{q}} \times D_{\mathbf{q}} \times & i\omega_{\mathbf{q},\lambda'} en_0 \delta(z) \\ -i\omega_{\mathbf{q},\lambda'} en_0 \delta(z) & n_0 m (\omega_{\mathbf{q},\lambda'}^2 - \beta^2 \mathbf{q} \otimes \mathbf{q}) \delta(z) \end{bmatrix} \begin{bmatrix} \mathbf{A}_{\mathbf{q},\lambda'}(z) \\ \mathbf{v}_{\mathbf{q},\lambda'} \end{bmatrix} = 0. \quad (\text{A4})$$

Taking the conjugate transpose of Eq. (A4), we obtain

$$\int dz [\mathbf{A}_{\mathbf{q},\lambda'}^\dagger(z), \mathbf{v}_{\mathbf{q},\lambda'}^\dagger] \begin{bmatrix} \omega_{\mathbf{q},\lambda'}^2 \epsilon_0 \bar{\epsilon}_d(z) - \frac{1}{\mu_0} D_{\mathbf{q}} \times D_{\mathbf{q}} \times & i\omega_{\mathbf{q},\lambda'} en_0 \delta(z) \\ -i\omega_{\mathbf{q},\lambda'} en_0 \delta(z) & n_0 m (\omega_{\mathbf{q},\lambda'}^2 - \beta^2 \mathbf{q} \otimes \mathbf{q}) \delta(z) \end{bmatrix} \begin{bmatrix} \mathbf{A}_{\mathbf{q},\lambda}(z) \\ \mathbf{v}_{\mathbf{q},\lambda} \end{bmatrix} = 0. \quad (\text{A5})$$

Subtracting this last equation from Eq. (A3), we obtain

$$\int dz [\mathbf{A}_{\mathbf{q},\lambda'}^\dagger(z), \mathbf{v}_{\mathbf{q},\lambda'}^\dagger] \begin{bmatrix} (\omega_{\mathbf{q},\lambda}^2 - \omega_{\mathbf{q},\lambda'}^2) \epsilon_0 \bar{\epsilon}_d(z) & i(\omega_{\mathbf{q},\lambda} - \omega_{\mathbf{q},\lambda'}) en_0 \delta(z) \\ -i(\omega_{\mathbf{q},\lambda} - \omega_{\mathbf{q},\lambda'}) en_0 \delta(z) & n_0 m (\omega_{\mathbf{q},\lambda}^2 - \omega_{\mathbf{q},\lambda'}^2) \delta(z) \end{bmatrix} \begin{bmatrix} \mathbf{A}_{\mathbf{q},\lambda}(z) \\ \mathbf{v}_{\mathbf{q},\lambda} \end{bmatrix} = 0. \quad (\text{A6})$$

If $\omega_{\mathbf{q},\lambda} \neq \omega_{\mathbf{q},\lambda'}$, we can divide by $\omega_{\mathbf{q},\lambda} - \omega_{\mathbf{q},\lambda'}$, obtaining one of the orthogonality conditions:

$$\int dz [\mathbf{A}_{\mathbf{q},\lambda'}^\dagger(z) \mathbf{v}_{\mathbf{q},\lambda'}^\dagger] \begin{bmatrix} (\omega_{\mathbf{q},\lambda} + \omega_{\mathbf{q},\lambda'})\epsilon_0 \bar{\epsilon}_d(z) & ien_0 \delta(z) \\ -ien_0 \delta(z) & n_0 m(\omega_{\mathbf{q},\lambda} + \omega_{\mathbf{q},\lambda'}) \delta(z) \end{bmatrix} \begin{bmatrix} \mathbf{A}_{\mathbf{q},\lambda}(z) \\ \mathbf{v}_{\mathbf{q},\lambda} \end{bmatrix} = 0. \quad (\text{A7})$$

We can obtain an additional orthogonality relation. If, in Eq. (A3), we replace $\mathbf{q} \rightarrow -\mathbf{q}$ and $\lambda \rightarrow \lambda'$, using the fact that $\omega_{\mathbf{q},\lambda} = \omega_{-\mathbf{q},\lambda}$, and take its conjugate complex, we obtain

$$\begin{bmatrix} \omega_{\mathbf{q},\lambda'}^2 \epsilon_0 \bar{\epsilon}_d(z) - \frac{1}{\mu_0} D_{\mathbf{q}} \times D_{\mathbf{q}} \times & -i\omega_{\mathbf{q},\lambda'} en_0 \delta(z) \\ i\omega_{\mathbf{q},\lambda'} en_0 \delta(z) & n_0 m(\omega_{\mathbf{q},\lambda'}^2 - \beta^2 \mathbf{q} \otimes \mathbf{q}) \delta(z) \end{bmatrix} \begin{bmatrix} \mathbf{A}_{-\mathbf{q},\lambda'}^*(z) \\ \mathbf{v}_{-\mathbf{q},\lambda'}^* \end{bmatrix} = 0. \quad (\text{A8})$$

We now contract this equation with $[\mathbf{A}_{\mathbf{q},\lambda}^\dagger(z) \mathbf{v}_{\mathbf{q},\lambda}^\dagger]$, integrate over z , and take its conjugate transpose, obtaining

$$\int dz [\mathbf{A}_{-\mathbf{q},\lambda'}^*(z) \mathbf{v}_{-\mathbf{q},\lambda'}^*] \begin{bmatrix} \omega_{\mathbf{q},\lambda'}^2 \epsilon_0 \bar{\epsilon}_d(z) - \frac{1}{\mu_0} D_{\mathbf{q}} \times D_{\mathbf{q}} \times & -i\omega_{\mathbf{q},\lambda'} en_0 \delta(z) \\ i\omega_{\mathbf{q},\lambda'} en_0 \delta(z) & n_0 m(\omega_{\mathbf{q},\lambda'}^2 - \beta^2 \mathbf{q} \otimes \mathbf{q}) \delta(z) \end{bmatrix} \begin{bmatrix} \mathbf{A}_{\mathbf{q},\lambda}(z) \\ \mathbf{v}_{\mathbf{q},\lambda} \end{bmatrix} = 0. \quad (\text{A9})$$

Contracting Eq. (A1) with $[\mathbf{A}_{-\mathbf{q},\lambda'}^t(z) \mathbf{v}_{-\mathbf{q},\lambda'}^t]$ and integrating over z we obtain

$$\int dz [\mathbf{A}_{-\mathbf{q},\lambda'}^t(z) \mathbf{v}_{-\mathbf{q},\lambda'}^t] \begin{bmatrix} \omega_{\mathbf{q},\lambda}^2 \epsilon_0 \bar{\epsilon}_d(z) - \frac{1}{\mu_0} D_{\mathbf{q}} \times D_{\mathbf{q}} \times & i\omega_{\mathbf{q},\lambda} en_0 \delta(z) \\ -i\omega_{\mathbf{q},\lambda} en_0 \delta(z) & n_0 m(\omega_{\mathbf{q},\lambda}^2 - \beta^2 \mathbf{q} \otimes \mathbf{q}) \delta(z) \end{bmatrix} \begin{bmatrix} \mathbf{A}_{\mathbf{q},\lambda}(z) \\ \mathbf{v}_{\mathbf{q},\lambda} \end{bmatrix} = 0. \quad (\text{A10})$$

Subtracting Eq. (A9) from (A10), we obtain

$$\int dz [\mathbf{A}_{-\mathbf{q},\lambda}^t(z) \mathbf{v}_{-\mathbf{q},\lambda}^t] \begin{bmatrix} (\omega_{\mathbf{q},\lambda}^2 - \omega_{\mathbf{q},\lambda'}^2) \epsilon_0 \bar{\epsilon}_d(z) & i(\omega_{\mathbf{q},\lambda} + \omega_{\mathbf{q},\lambda'}) en_0 \delta(z) \\ -i(\omega_{\mathbf{q},\lambda} + \omega_{\mathbf{q},\lambda'}) en_0 \delta(z) & n_0 m(\omega_{\mathbf{q},\lambda}^2 - \omega_{\mathbf{q},\lambda'}^2) \delta(z) \end{bmatrix} \begin{bmatrix} \mathbf{A}_{\mathbf{q},\lambda}(z) \\ \mathbf{v}_{\mathbf{q},\lambda} \end{bmatrix} = 0. \quad (\text{A11})$$

For $\omega_{\mathbf{q},\lambda} + \omega_{\mathbf{q},\lambda'} \neq 0$, we obtain a second orthogonality condition:

$$\int dz [\mathbf{A}_{-\mathbf{q},\lambda}^t(z) \mathbf{v}_{-\mathbf{q},\lambda}^t] \begin{bmatrix} (\omega_{\mathbf{q},\lambda} - \omega_{\mathbf{q},\lambda'}) \epsilon_0 \bar{\epsilon}_d(z) & ien_0 \delta(z) \\ -ien_0 \delta(z) & n_0 m(\omega_{\mathbf{q},\lambda} - \omega_{\mathbf{q},\lambda'}) \delta(z) \end{bmatrix} \begin{bmatrix} \mathbf{A}_{\mathbf{q},\lambda}(z) \\ \mathbf{v}_{\mathbf{q},\lambda} \end{bmatrix} = 0. \quad (\text{A12})$$

2. Hamiltonian in terms of mode amplitudes

We now insert the expansion of the fields in terms of mode functions, Eqs. (31) and (32), into the classical Hamiltonian (30). Using Eqs. (28) and (29), we can write

$$H = \frac{1}{2} \sum_{\mathbf{q},\lambda,\lambda'} [h_{\lambda,\lambda'}(\mathbf{q}) \alpha_{\mathbf{q},\lambda'}^*(t) \alpha_{\mathbf{q},\lambda}(t) + \tilde{h}_{\lambda,\lambda'}(\mathbf{q}) \alpha_{-\mathbf{q},\lambda'}(t) \alpha_{\mathbf{q},\lambda}(t)] + \text{c.c.}, \quad (\text{A13})$$

where

$$h_{\lambda,\lambda'}(\mathbf{q}) = \int dz [\mathbf{A}_{\mathbf{q},\lambda'}^\dagger(z) \mathbf{v}_{\mathbf{q},\lambda'}^\dagger] \times \begin{bmatrix} \omega_{\mathbf{q},\lambda'} \omega_{\mathbf{q},\lambda} \epsilon_0 \bar{\epsilon}_d(z) + \mu_0^{-1} D_{\mathbf{q}} \times D_{\mathbf{q}} & 0 \\ 0 & \delta(z) (n_0 m \omega_{\mathbf{q},\lambda'} \omega_{\mathbf{q},\lambda} + n_0 m \beta^2 \mathbf{q} \otimes \mathbf{q}) \end{bmatrix} \begin{bmatrix} \mathbf{A}_{\mathbf{q},\lambda}(z) \\ \mathbf{v}_{\mathbf{q},\lambda} \end{bmatrix}, \quad (\text{A14})$$

$$\tilde{h}_{\lambda,\lambda'}(\mathbf{q}) = \int dz [\mathbf{A}_{-\mathbf{q},\lambda'}^t(z) \mathbf{v}_{-\mathbf{q},\lambda'}^t] \begin{bmatrix} -\omega_{\mathbf{q},\lambda'} \omega_{\mathbf{q},\lambda} \epsilon_0 \bar{\epsilon}_d(z) + \mu_0^{-1} D_{\mathbf{q}} \times D_{\mathbf{q}} & 0 \\ 0 & \delta(z) (-n_0 m \omega_{\mathbf{q},\lambda'} \omega_{\mathbf{q},\lambda} + n_0 m \beta^2 \mathbf{q} \otimes \mathbf{q}) \end{bmatrix} \begin{bmatrix} \mathbf{A}_{\mathbf{q},\lambda}(z) \\ \mathbf{v}_{\mathbf{q},\lambda} \end{bmatrix}. \quad (\text{A15})$$

Using the mode-function equation (A1), we can write

$$h_{\lambda,\lambda'}(\mathbf{q}) = \omega_{\mathbf{q},\lambda} \int dz [\mathbf{A}_{\mathbf{q},\lambda'}^\dagger(z) \mathbf{v}_{\mathbf{q},\lambda'}^\dagger] \begin{bmatrix} (\omega_{\mathbf{q},\lambda'} + \omega_{\mathbf{q},\lambda}) \epsilon_0 \bar{\epsilon}_d(z) & ien_0 \delta(z) \\ -ien_0 \delta(z) & \delta(z) n_0 m (\omega_{\mathbf{q},\lambda'} + \omega_{\mathbf{q},\lambda}) \end{bmatrix} \begin{bmatrix} \mathbf{A}_{\mathbf{q},\lambda}(z) \\ \mathbf{v}_{\mathbf{q},\lambda} \end{bmatrix}, \quad (\text{A16})$$

$$\tilde{h}_{\lambda,\lambda'}(\mathbf{q}) = \omega_{\mathbf{q},\lambda} \int dz [\mathbf{A}_{-\mathbf{q},\lambda'}^t(z) \mathbf{v}_{-\mathbf{q},\lambda'}^t] \begin{bmatrix} (\omega_{\mathbf{q},\lambda} - \omega_{\mathbf{q},\lambda'}) \epsilon_0 \bar{\epsilon}_d(z) & ien_0 \delta(z) \\ -ien_0 \delta(z) & \delta(z) n_0 m (\omega_{\mathbf{q},\lambda} - \omega_{\mathbf{q},\lambda'}) \end{bmatrix} \begin{bmatrix} \mathbf{A}_{\mathbf{q},\lambda}(z) \\ \mathbf{v}_{\mathbf{q},\lambda} \end{bmatrix}. \quad (\text{A17})$$

Using the orthogonality condition (A12) we conclude that $\tilde{h}_{\lambda,\lambda'}(\mathbf{q}) = 0$. The orthogonality condition (A7) implies that $h_{\lambda,\lambda'}(\mathbf{q}) = 0$, except when $\lambda = \lambda'$ (assuming there are no degeneracies in $\omega_{\mathbf{q},\lambda}$). Therefore, we see that the classical Hamiltonian can be written as in Eq. (41), with the mode normalization constant being given by

$$N_{\mathbf{q},\lambda} = \frac{1}{2\epsilon_0 \omega_{\mathbf{q},\lambda}^2} \int dz [\mathbf{A}_{\mathbf{q},\lambda}^\dagger(z) \mathbf{v}_{\mathbf{q},\lambda}^\dagger] \begin{bmatrix} 2\omega_{\mathbf{q},\lambda}^2 \epsilon_0 \bar{\epsilon}_d(z) & i\omega_{\mathbf{q},\lambda} en_0 \delta(z) \\ -i\omega_{\mathbf{q},\lambda} en_0 \delta(z) & 2\omega_{\mathbf{q},\lambda}^2 \delta(z) n_0 m \end{bmatrix} \begin{bmatrix} \mathbf{A}_{\mathbf{q},\lambda}(z) \\ \mathbf{v}_{\mathbf{q},\lambda} \end{bmatrix}, \quad (\text{A18})$$

which can be written as Eq. (42).

APPENDIX B: REFLECTION COEFFICIENTS OF GRAPHENE STRUCTURES

In this Appendix we provide the reflection coefficients used in the evaluation of the loss function, Eq. (74), and in the evaluation of the full decay rate of a quantum emitter, Eq. (83).

1. Reflection coefficients for a single graphene layer

The Fresnel problem for a single graphene sheet has been considered in Ref. [55]. Therefore, we provide here the final results only and for simplicity we assume we are dealing with nonmagnetic media. For an incoming wave from region 2, and for the s polarization, the reflection and transmission coefficient read

$$r_s = \frac{k_{z,2} - k_{z,1} - \mu_0 \omega \sigma_{g,T}}{k_{z,2} + k_{z,1} + \mu_0 \omega \sigma_g}, \quad (\text{B1})$$

$$t_s = \frac{2k_{z,2}}{k_{z,2} + k_{z,1} + \mu_0 \omega \sigma_{g,T}}, \quad (\text{B2})$$

whereas for the p polarization we have

$$r_p = -\frac{\epsilon_2 k_{z,1} - \epsilon_1 k_{z,2} - k_{z,1} k_{z,2} \sigma_{g,L} / (\omega \epsilon_0)}{\epsilon_2 k_{z,1} + \epsilon_1 k_{z,2} + k_{z,1} k_{z,2} \sigma_{g,L} / (\omega \epsilon_0)}, \quad (\text{B3})$$

$$t_p = \sqrt{\frac{\epsilon_1}{\epsilon_2}} \frac{2k_{z,2} \epsilon_1}{\epsilon_2 k_{z,1} + \epsilon_1 k_{z,2} + k_{z,1} k_{z,2} \sigma_{g,L} / (\omega \epsilon_0)}. \quad (\text{B4})$$

In these equations, we have $k_{z,n} = \sqrt{\epsilon_n \omega^2 / c^2 - q^2} = ik_n$, and $\sigma_{g,L/T}$ is the optical longitudinal (L) and transverse (T) conductivity of graphene, ϵ_0 and μ_0 are the vacuum permittivity and permeability, respectively, q is the wave number along the

graphene sheet, and ω is the frequency of the electromagnetic radiation.

2. Graphene-metal reflectance coefficient

The reflection coefficient for the p polarization for this structure is given by

$$r_p = 1 - \frac{2k_{z,1} k_2^2 \sin(k_{z,1} d)}{k_{z,1} \sin(k_{z,1} d) (k_{z,2} \mu_0 \omega \sigma_{g,L} + k_2^2) + ik_{z,2} k_1^2 \cos(k_{z,1} d)}, \quad (\text{B5})$$

where $k_n^2 = \epsilon_n \omega^2 / c^2$, d is the graphene-metal distance, and $\kappa_n^2 = k_n^2 - q^2$, where q is the wave number along the graphene sheet. For the s polarization we have

$$r_s = -1 + \frac{2k_{z,2} \sin(k_{z,1} d)}{\sin(k_{z,1} d) (k_{z,2} + \mu_0 \omega \sigma_{g,T}) + ik_{z,1} \cos(k_{z,1} d)}. \quad (\text{B6})$$

APPENDIX C: GRAPHENE DRUDE CONDUCTIVITY

In order to take into account the effects of Ohmic losses, the conductivity of graphene is modified by adding a relaxation rate or broadening factor, γ , to Eqs. (37) and (38), such that the conductivities now read

$$\sigma_{g,T}^{\text{lossy}}(\mathbf{q}, \omega) = D \frac{i}{\omega + i\gamma}, \quad (\text{C1})$$

$$\sigma_{g,L}^{\text{lossy}}(\mathbf{q}, \omega) = D \frac{i\omega}{\omega^2 + i\omega\gamma - \beta^2 q^2}, \quad (\text{C2})$$

where D is the Drude weight. The local form of the conductivity is obtained by taking $\beta = 0$. This lossy form of the conductivity is used in Eqs. (74) and (83).

[1] G. S. Agarwal, *Quantum Optics*, 1st ed. (Cambridge University Press, Cambridge, UK, 2013).

[2] R. W. Heeres, L. P. Kouwenhoven, and V. Zwiller, *Nat. Nanotechnol.* **8**, 719 (2013).

[3] Z. Jacob, *MRS Bull.* **37**, 761 (2012).

[4] M. S. Tame, K. R. McEnery, S. K. Ozdemir, J. Lee, S. A. Maier, and M. S. Kim, *Nat. Phys.* **9**, 329 (2013).

[5] D. Martín-Cano, P. A. Huidobro, E. Moreno, and F. J. García-Vidal, in *Modern Plasmonics*, 1st ed., edited by A. A. Maradudin, J. R. Sambles, and W. L. Barnes (Elsevier, New York, 2014), Vol. 4, Chap. 12, p. 349.

[6] J. S. Fakonas, A. Mitykova, and H. A. Atwater, *New J. Phys.* **17**, 023002 (2015).

[7] J. M. Fitzgerald, P. Narang, R. V. Craster, S. A. Maier, and V. Giannini, *Proc. IEEE* **104**, 2307 (2016).

[8] M.-C. Dheur, E. Devaux, T. W. Ebbesen, A. Baron, J.-C. Rodier, J.-P. Hugonin, P. Lalanne, J.-J. Greffet, G. Messin, and F. Marquier, *Sci. Adv.* **2**, e1501574 (2016).

[9] S. Bozhevolnyi and N. Mortensen, *Nanophotonics* **6**, 1185 (2017).

[10] D. Xu, X. Xiong, L. Wu, X.-F. Ren, C. E. Png, G.-C. Guo, Q. Gong, and Y.-F. Xiao, *Adv. Opt. Photon.* **10**, 703 (2018).

[11] A. I. Fernández-Domínguez, S. I. Bozhevolnyi, and N. A. Mortensen, *ACS Photon.* **5**, 3447 (2018).

[12] L. Ju, B. Geng, J. Horng, C. Girit, M. Martin, Z. Hao, H. A. Bechtel, X. Liang, A. Zettl, Y. R. Shen, and F. Wang, *Nat. Nanotechnol.* **6**, 630 (2011).

[13] Z. Fei, G. O. Andreev, W. Bao, L. M. Zhang, A. S. McLeod, C. Wang, M. K. Stewart, Z. Zhao, G. Dominguez, M. Thiemens, M. M. Fogler, M. J. Tauber, A. H. Castro-Neto, C. N. Lau, F. Keilmann, and D. N. Basov, *Nano Lett.* **11**, 4701 (2011).

[14] Z. Fei, A. S. Rodin, G. O. Andreev, W. Bao, A. S. McLeod, M. Wagner, L. M. Zhang, Z. Zhao, M. Thiemens, G. Dominguez, M. M. Fogler, A. H. C. Neto, C. N. Lau, F. Keilmann, and D. N. Basov, *Nature (London)* **487**, 82 (2012).

[15] J. Chen, M. Badioli, P. Alonso-González, S. Thongrattanasiri, F. Huth, J. Osmond, M. Spasenović, A. Centeno, A. Pesquera, P. Godignon, A. Zurutuza Elorza, N. Camara, F. J. G. de Abajo, R. Hillenbrand, and F. H. L. Koppens, *Nature (London)* **487**, 77 (2012).

[16] A. Woessner, M. B. Lundberg, Y. Gao, A. Principi, M. Carrega, K. Watanabe, T. Taniguchi, G. Vignale, M. Polini, J. Hone, R. Hillenbrand, and F. H. L. Koppens, *Nat. Mater.* **14**, 421 (2015).

[17] G. W. Hanson, S. A. Hassani Gangaraj, C. Lee, D. G. Angelakis, and M. Tame, *Phys. Rev. A* **92**, 013828 (2015).

[18] I. Alonso Calafell, J. D. Cox, M. Radonjić, J. R. M. Saavedra, F. J. García de Abajo, L. A. Rozema, and P. Walther, *npj Quantum Inf.* **5**, 37 (2019).

- [19] D. Alcaraz Iranzo, S. Nanot, E. J. C. Dias, I. Epstein, C. Peng, D. K. Efetov, M. B. Lundeberg, R. Parret, J. Osmond, J.-Y. Hong, J. Kong, D. R. Englund, N. M. R. Peres, and F. H. L. Koppens, *Science* **360**, 291 (2018).
- [20] M. B. Lundeberg, Y. Gao, R. Asgari, C. Tan, B. Van Duppen, M. Autore, P. Alonso-González, A. Woessner, K. Watanabe, T. Taniguchi, R. Hillenbrand, J. Hone, M. Polini, and F. H. L. Koppens, *Science* **357**, 187 (2017).
- [21] E. J. C. Dias, D. A. Iranzo, P. A. D. Gonçalves, Y. Hajati, Y. V. Bludov, A.-P. Jauho, N. A. Mortensen, F. H. L. Koppens, and N. M. R. Peres, *Phys. Rev. B* **97**, 245405 (2018).
- [22] D. E. Chang, A. S. Sørensen, P. R. Hemmer, and M. D. Lukin, *Phys. Rev. Lett.* **97**, 053002 (2006).
- [23] F. Alpeggiani and L. C. Andreani, *Plasmonics* **9**, 965 (2014).
- [24] V. G. Bordo, *J. Opt. Soc. Am. B* **36**, 323 (2019).
- [25] B. A. Ferreira and N. M. R. Peres, *Europhys. Lett.* **127**, 37002 (2019).
- [26] J. J. Hopfield, *Phys. Rev.* **112**, 1555 (1958).
- [27] A. I. Alekseev and Yu. P. Nikitin, *J. Exptl. Theoret. Phys. (USSR)* **50**, 915 (1966) [*Sov. Phys. JETP* **23**, 608 (1966)].
- [28] G. S. Agarwal, *Phys. Rev. A* **11**, 230 (1975).
- [29] B. Huttner and S. M. Barnett, *Phys. Rev. A* **46**, 4306 (1992).
- [30] P. Milonni, *J. Mod. Opt.* **42**, 1991 (1995).
- [31] T. Gruner and D.-G. Welsch, *Phys. Rev. A* **51**, 3246 (1995).
- [32] T. Gruner and D.-G. Welsch, *Phys. Rev. A* **53**, 1818 (1996).
- [33] R. Matloob, R. Loudon, S. M. Barnett, and J. Jeffers, *Phys. Rev. A* **52**, 4823 (1995).
- [34] H. T. Dung, L. Knöll, and D.-G. Welsch, *Phys. Rev. A* **57**, 3931 (1998).
- [35] T. G. Philbin, *New J. Phys.* **12**, 123008 (2010).
- [36] Z. Allameh, R. Roknizadeh, and R. Masoudi, *Plasmonics* **11**, 875 (2016).
- [37] W. E. I. Sha, A. Y. Liu, and W. C. Chew, *IEEE J. Multiscale Multiphys. Comput. Tech.* **3**, 198 (2018).
- [38] C. K. Carniglia and L. Mandel, *Phys. Rev. D* **3**, 280 (1971).
- [39] C. K. Carniglia, L. Mandel, and K. H. Drexhage, *J. Opt. Soc. Am. A* **62**, 479 (1972).
- [40] P. Gossel, J.-M. Vigoureux, and R. Payen, *Can. J. Phys.* **55**, 1259 (1977).
- [41] L. D. Landau and E. M. Lifshitz, *Electrodynamics of Continuous Media*, 2nd ed., Course of Theoretical Physics (Pergamon Press, Oxford, UK, 1984).
- [42] M. Agu, *Jpn. J. Appl. Phys.* **18**, 2143 (1979).
- [43] A. J. Chaves, N. M. R. Peres, G. Smirnov, and N. A. Mortensen, *Phys. Rev. B* **96**, 195438 (2017).
- [44] A. L. Fetter, *Ann. Phys. (NY)* **81**, 367 (1973).
- [45] R. Ruppin, *Phys. Lett. A* **299**, 309 (2002).
- [46] B. Amorim and A. J. Chaves (unpublished).
- [47] T. Christensen, *From Classical to Quantum Plasmonics in Three and Two Dimensions* (Springer, Berlin, 2017).
- [48] Y. O. Nakamura, *Prog. Theor. Phys.* **70**, 908 (1983).
- [49] A. Lucas and K. C. Fong, *J. Phys.: Condens. Matter* **30**, 053001 (2018).
- [50] We point out that Eqs. (37) and (38) can also be obtained as a small momentum approximation to the conductivity of a metal obtained from the semiclassical Boltzmann equation. The same result can also be obtained from the quantum Kubo formula for the conductivity, within a small momentum approximation and neglecting interband contributions.
- [51] The Drude conductivity is also recovered in the $\mathbf{q} \rightarrow 0$ limit.
- [52] Although not explicitly given, the normalization constant in Ref. [17], where it is written as $N_{\mathbf{k}}$, is given by $N_{\mathbf{q},\text{sp}} = \epsilon_d \int dz |\mathbf{A}_{\mathbf{q},\text{sp}}(z)|^2 + \frac{|\sigma''| - \sigma''}{2\epsilon_0 \omega_{\mathbf{q},\text{sp}}} |\mathbf{A}_{\mathbf{q},\text{sp}}^{\parallel}(0)|^2$, where σ'' is the imaginary part of the conductivity of graphene and $\mathbf{A}_{\mathbf{q},\text{sp}}^{\parallel}(z)$ are the in-plane components of the mode function. However, we point out that neglecting losses and if we model the conductivity of graphene by a local Drude formula, $\sigma(\omega) = iD/\omega$, then both the above expression and Eq. (48) for the transverse plasmon reduce to $N_{\mathbf{q},\text{sp}} = \int dz \epsilon_d(z) |\mathbf{A}_{\mathbf{q},\text{sp}}(z)|^2$.
- [53] M. Jablan, H. Buljan, and M. Soljagic, *Phys. Rev. B* **80**, 245435 (2009).
- [54] Y. V. Bludov, A. Ferreira, N. M. R. Peres, and M. I. Vasilevskiy, *Int. J. Mod. Phys. B* **27**, 1341001 (2013).
- [55] P. A. D. Gonçalves and N. M. R. Peres, *An Introduction to Graphene Plasmonics* (World Scientific, Singapore, 2016).
- [56] L. Novotny and B. Hecht, *Principle of Nano-Optics* (Cambridge University Press, New York, 2006).
- [57] A. Archambault, F. Marquier, J.-J. Greffet, and C. Arnold, *Phys. Rev. B* **82**, 035411 (2010).
- [58] G. S. Agarwal, *Phys. Rev. A* **12**, 1475 (1975).
- [59] F. H. L. Koppens, D. E. Chang, F. J. García De Abajo, and F. J. G. D. Abajo, *Nano Lett.* **11**, 3370 (2011).